TAMPEREEN TEKNILLINEN YLIOPISTO
TAMPERE UNIVERSITY OF TECHNOLOGY

PASI SEPPÄLÄ

ELECTRICAL PERFORMANCE OF CARBON-BASED HYBRID FILLER SYSTEMS IN THERMOPLASTIC POLYMER BLENDS

Master of Science thesis

Examiner: Asst. Prof. Essi Sarlin
Examiner and topic approved by the
Faculty Council of the Faculty of
Engineering sciences
on 1st of Februry 2017

ABSTRACT

PASI SEPPÄLÄ: Electrical performance of carbon-based hybrid filler systems in thermoplastic polymer blends
Tampere University of Technology
Master of Science thesis, 60 pages, 5 Appendix pages
August 2017
Master's Degree Programme in Materials Engineering
Major: Materials technology
Examiner: Asst. Prof. Essi Sarlin
Keywords: Electrical properties, Electrical percolation, Hybrid filler system, Polymer blend, Thermoplastic

Accumulation of static electricity causes danger in applications where non-conductive materials are subjected to repetitive contact with charged particles. Charged object upon contact with a conductive surface causes an electric shock, which can be destructive. By using materials with different electrical conductivities, protection against various electrical phenomena can be obtained. Well conductive materials are suitable to protect sensitive devices from electromagnetic interference, while moderately conductive materials provide more controlled charge transfer.

This thesis aimed to review the factors that contribute to the formation of electrical properties in thermoplastic polymeric blends, and to find out if hybrid filler systems could be applied for more delicate tailoring of the final properties. Besides the focus on electrical properties, other crucial elements were briefly considered. In the experimental part 6 different fillers were compounded and tested in two polymeric blends with fixed constitutions. The fillers consist of carbon's allotropes, e.g. carbon black. The electrical percolation curves for the materials were formed with surface resistance measurements from extruded and injection moulded specimens. Further analysis was carried out with differential scanning calorimetry (DSC), scanning electron microscopy (SEM) and thermoforming. The filler contents were verified with ash content measurements from the produced compounds.

According to the results, with injection moulding the transition from insulative to conductive occurred within narrower region, when compared to the extruded materials. The observed differences between the injection moulded and extruded specimens' behaviours could be due to the differences in blend morphologies, thus further experimentation is necessary to point out the main factors and their influence. A decrease in the degree of crystallinity was found to increase the percolation threshold and overall resistivity for the experimented specimens.

TIIVISTELMÄ

PASI SEPPÄLÄ: Hiilipohjaisten hybriditäyteaineiden käytettävyys sähköä johtavissa kestomuoviseoksissa
Tampereen teknillinen yliopisto
Diplomityö, 60 sivua, 5 liitesivua
Elokuu 2017
Materiaalitekniikan DI-tutkinto-ohjelma
Pääaine: Materiaaliteknologia
Tarkastajat: Assistant prof. Essi Sarlin
Avainsanat: Sähköiset ominaisuudet, sähköinen perkolaatio, hybriditäyteaine, Polymeeriseos, kestomuovi

Kun kaksi eristävää materiaalia hankaavat toisiaan vasten, niiden välille syntyy sähköinen epätasapaino, jota kutsutaan kansankielellä staattiseksi sähköksi. Staattisen varautumisen aiheuttamat sähköiskut ovat usein haitallisia, mutta pahimmillaan ne voivat olla jopa hengenvaarallisia. Sähköä johtavat materiaalit eivät varaudu staattisesti. Hyvin johtavia materiaaleja käytetään myös suojaamaan esimerkiksi sähkömagneettiselta interferenssiltä.

Tämän diplomityön teoriaosan tarkoituksena on monipuolisesti käsitellä täyteaineistetun muoviseoksen sähkönjohtavuuteen vaikuttavia tekijöitä. Teoriaosassa esitellään muovien sähkönjohtavuus yleisesti, minkä jälkeen syvennytään täyteaineistettuihin muoviseoksiin. Sähkönjohtavuuteen vaikuttavia tekijöitä käsitellään kussakin kappaleessa painottaen joko matriisin, täyteaineen tai prosessoinnin osuutta kokonaisuuteen. Kokeellisessa osassa tutkitaan kuutta hiilipohjaista täyteainetta kahdessa eri muoviseoksessa. Prosessointimenetelminä materiaaleille käytettiin ruiskuvalua tai ekstruusiota. Materiaalit laimennettiin kuivaseoksin eri täyteainepitoisuuksiin, ja niistä mitattiin pintavastukset. Osasta materiaaleja tutkittiin myös lämpömuovauksen vaikutusta sähkönjohtavuuteen. Analyysin tueksi näytteitä kuvattiin pyyhkäisyelektronimikroskoopilla (SEM) sekä osasta määritettiin kiteisyysaste differentiaalisella pyyhkäisykalorimetrillä (DSC).

Tämän työn perusteella voidaan todeta, että polymeeriseoksia ja hybriditäyteaineita vertaillessa on haasteellista varioida parametreja siten, että voidaan yksiselitteisesti todeta vaikutuksen taustalla olevaa mekanismia. Mittauksista havaittiin, että ruiskuvaletut hybriditäyteaineistetut materiaalit muuttuivat ekstruusiolla valmistettuihin materiaaleihin verrattuna pienemmällä täyteainelisäyksellä sähköisesti eristävästä johtavaksi. Kiteisyysasteen havaittiin olevan käänteisesti verrannollinen perkolaatiopitoisuuteen ja resistiivisyyteen tutkituilla materiaaleilla.

PREFACE

The past seven months have kept me busy, but finally it seems to be over. Within the time period there has been times when the progression of the thesis seemed to be non-existent, but somehow the workload diminished by taking small bites and a couple of baby steps. Thus I would like to show my appreciation for the different parties that have offered me help and guidance when needed:

Foremost I'd like to thank Premix Oy for giving me the opportunity to carry out my thesis with objectives that have inspired and kept me motivated. From Premix Oy, I'd like to thank especially M.Sc. Kari Alha and M.Sc. Lauri Laaksonen for their guidance. I would also like to thank the R&D Technician Jari Hinkkanen, for his help on the plastic processing and the other related issues.

From the Technical University of Tampere, I give my gratitude for Asst. prof. Essi Sarlin for being the instructor for this thesis. I'd like to thank the whole research group of Plastics and Elastomer Technology for providing me a supportive network for my studies.

The fact that I could successfully stick to my schedule is largely thanks to my wife for showing me what diligent working means. Thanks to your encouragement, I did not fail nor did I feel like I couldn't make it to the end. Lastly, I would like to thank my family and friends for being so great.

Tampere, 02.08.2017

Pasi Seppälä

TABLE OF CONTENTS

LIST OF ABBREVIATIONS AND SYMBOLS

ASTM	American Society for Testing and Materials
ANSI	American National Standards Institute
CB	Carbon black
CF	Carbon fiber
CNF	Carbon nanofiber
CNT	Carbon nanotube
CRT	Cathode ray tube
DSC	Differential scanning calorimetry
ESD	Electrostatic discharge
EVA	Poly(ethylene-vinyl acetate)
HDPE	High density poly(ethylene)
HIPS	High impact poly(styrene)
i-PP	Isotactic poly(propylene)
ICP	Inherently conductive polymer
LDPE	Low density poly(ethylene)
LLDPE	Linear low density poly(ethylene)
MWCNT	Multi-walled carbon nanotube
N###	Carbon black grade, # stands for any number
NTC	Negative temperature coefficient
NR	Natural rubber
PMMA	Poly(methyl methacrylate)
PP	Poly(propylene)
PS	Poly(styrene)
PTC	Positive temperature coefficient
SFE	Surface free energy
SEM	Scanning electron microscopy
SR	Surface resistance
TEM	Transmission electron microscopy
UHMWPE	Ultra high molecular weight poly(ethylene)
VPCF	Vapour grown carbon fiber
XPS	X-ray photoelectron spectroscopy

α	Filler diameter ratio
γ	Surface energy, Surface tension
$\dot{\gamma}$	Shear strain rate
γ_{i-j}	Surface energy between phases i and j

Δ	Prefix indicating a change in property
ΔH_i	Enthalpy of a reaction
λ	Aspect ratio
μ	Power law exponent
π-bond	Covalent bond that occurs through p-orbitals
ρ_s	Surface resistivity
σ	DC conductivity
σ_0	DC conductivity above percolation threshold
σ-bond	Symmetrical covalent bond
τ	Time between particle collisions
Φ_i	Volume fraction
Φ_c	Volume fraction at percolation threshold
Φ_i^{th}	Percolation threshold of a spherical particle
Φ_j^{th}	Percolation threshold of a cylindrical particle
ω_{i-j}	Wetting coefficient
A/B	Annotation for a blend consisting of A and B
$A+B$	Annotation for hybrid filler system of A and B
B_c	Amount of particle contacts on a single particle
d_i	Diameter of a spherical particle
d_j	Diameter of a cylindrical particle
D	Width of an electrode
e	Particle charge
E_g	Energy band gap
$F(E_g)$	Probability of fermi-dirac function
H_2O	Chemical formula for water
I_s	Surface current
k	Proportionality factor
k_b	Boltzmann's constant
L	Distance between electrodes
m	Mass
m_i	Weight fraction of component i
n_e	Number of electrons per unit volume
N	Number of atoms
N_c	Critical concentration of a filler, see percolation threshold
$P_{c,i}$	Percolation threshold of component i
sp^2	Type of a molecular orbital hybridization
T	Temperature in kelvins
U	Measurement voltage
$\langle V \rangle$	Average excluded volume
$\langle V_{ex} \rangle$	Total excluded volume
V_{unit}	Amount of particles per unit volume

Part I

Theoretical background

1. INTRODUCTION

The incorporation of conductive fillers into polymers has led to a material class called conductive plastics. These plastics are composite materials, which exhibit the good characteristics of plastics e.g. low weight and ease of processing complex shapes accompanied with electrical conductivity - the known property of metals. The degree of conductivity defines the possible end applications. Moderately conductive, i.e. dissipative materials, protect sensitive components by hindering the accumulation of static charge, whereas highly conductive materials can also be used e.g. to minimize signal losses caused by electromagnetic interference.

From the manufacturer point of view it is essential to know how the properties are dependent upon different parameters in order to provide the market with a good quality product, that fits the product specifications. The aim in the experimental part is to assess the potential of hybrid filler systems in a certain industrial application. In other words, the aim would be to find material combinations or knowledge, that would improve the controllability of material properties within the dissipative region i.e. the region of sustained conductivity. The theoretical part of this thesis attempts to include various aspects related to conductive polymers with only two major boundaries in its scope: Firstly the thesis assesses only thermoplastic matrix materials, and secondly, only carbon-based fillers are considered despite the fact that metallic fillers exhibit great conducting characteristics. In the experimental part only two chosen polymeric blends with six specific fillers are studied with a clear focus on the dissipative region i.e. the region of sustained conductivity.

The need for understanding and improvement of electrically conductive materials is high due to the potential, even deadly, risks related to of static charging. But it is also important to improve the materials to keep up with the technology driven world as the fossil fuels are depleting and regulations get stricter on yearly basis. By using conductive high performance materials the risks related to electricity can be subdued while increasing the products' performance. For products without absolute need for better electrical properties, it all comes down to monetary issues. By developing the craft of conductive plastics the prices could be lowered and even new innovations can be found.

2. ELECTRICAL PROPERTIES OF POLYMERS

Conductivity σ is a solid state material property, which can be represented according to free electron model of conductivity as

$$\sigma = \frac{n_e \, e^2 \tau}{m} \tag{2.1}$$

where n_e is the number of electrons per unit volume, e is the particle charge, τ is the time between collisions and m is particle mass. To work properly, this expression of conductivity needs quantum mechanical considerations in defining the scattering rate. [1, p.621-622] The main factors, which account for conductivity as stated in **eq.** 2.1 are carrier concentration, their mobility and the unit of charge [2, p.593].

The conductive behaviour is often described with a band model of solids. According to the model, when N atoms are brought together to form a solid, the total potential energy of system is split into N energy levels. Due to the stochastic nature of particles, energy bands are formed. The bands consist of different levels of potential energy that are close to each other. Electrons are known to locate on different electron shells, which leads to band gaps. The highest energy band containing electrons is known as valence band or conduction band. The former term is used in the case of completely filled bands while the latter is used only for the partially filled bands. Whether the solid is insulator, conductor or a semiconductor depends on the electron configuration and the band gap E_g between the conduction band and the lower energy band. If E_g exists and is low enough, the material is considered to be an intrinsic semiconductor. [1, p.632-633]

Resistivity is the reciprocal of conductivity, and for a semiconductor at room temperature it varies between $10^{-3} - 10^{9}$ Ωcm [2, p. 575]. Semiconducting materials can be characterized by determining the probability of finding a charged particle in the middle of the band gap, that is according to a Fermi-Dirac function

$$F(E_g) \; = \; \frac{e^{E_g}}{2k_b T} \tag{2.2}$$

where k_b is the Boltzmann constant and T is temperature in kelvins. As the equation states, lower band gap energy and higher temperature leads to increased conductivity in semiconductors. For example the amount of mobile electrons increases for graphite when temperature is increased, and thus it becomes more conductive. For conducting materials a decrease in conductivity is observed upon the increase of temperature due to higher amount of lattice vibrations that obstruct the movement of electrons [1, p.635].

The materials that are used in electronic applications are typically categorized in relation to their resistivity. One possible categorization is given in **table** 2.1 [3, p. 16]. However, there are slight nuances in the definitions depending on the used reference. According to EIA standards, a material with surface resistance less than $10^5\ \Omega/sq$ is conductive, greater than $10^{12}\ \Omega/sq$ is insulative – Those in between are characterized as dissipative [4, p. 209].

Table 2.1 *Classification according to volume resistivity of a material [3, p. 16].*

Type	**Range**
Insulative	10^{14} *to* $10^{12}\ \Omega.cm$
Antistatic	10^{12} *to* $10^{9}\ \Omega.cm$
Dissipative	10^{8} *to* $10^{6}\ \Omega.cm$
Conductive	10^{6} *to* $10^{-1}\ \Omega.cm$

The terms in **table** 2.1 describe the materials' ability to transfer electrical charge throughout the material. Insulative materials are poor charge carriers, that can be used in applications such as wire coatings. Antistatic materials are able to transfer limited amount of charge, which is often applied in prevention of static charge accumulation. Dissipative materials are able to transfer charge in an efficient yet controlled fashion, whereas conductive materials offer electrical conductivity similar to metals.

2.1 Inherently conductive polymers, ICP

Polymers are long molecules formed by covalent bonding. Their lack of free charge carriers is the main cause for the difference between polymeric and metallic conductivity. With the use of engineering techniques and specific constitutions, conductive pathways can be achieved despite the insulating features of polymeric materials. It is possible to enhance the conductivity of the polymer component itself or to introduce a conductive additive, which makes the system extrinsically conductive.

Polymeric structure that contains conjugated double bonds provides a mechanism for charge transportation. The double bonds are formed between atoms by σ-bond and π-bond. The former is a bond between the electrons on sp^2-hybridized molecular orbitals. The electrons on p-orbitals form weaker π-bonds, which in conjugated structures lead to resonance stabilization and de-localization of electrons. The movement of these electrons is less restricted, thus they are able to drift along the conjugated chain making the structure able to transfer charge. ICPs can have either aliphatic or aromatic chemical structures, of which the structures of poly(acetylene) and poly(p-phenylene) are shown in **figure** 2.1 as examples.

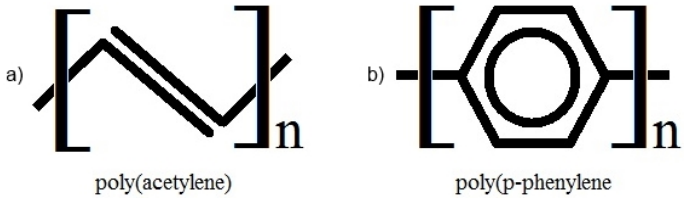

Figure 2.1 *Examples of a) aliphatic and b) aromatic structures.*

The π-bonds of ICPs are susceptible to oxidation and reduction reactions, for which reason a process called doping is often applied for enhancing conductivity. Since the charge mobility conditions are excellent for ICPs, the intuitive way to enhance the conductivity is by increasing the amount of free charge carriers. As an example pristine poly(acetylene) is a semiconductor with E_g of $1,5\ eV$ and conductivity of $\approx 10^{-10}\ Scm^{-1}$. By doping it with iodine a remarkable increase of conductivity up to $10^4\ Scm^{-1}$ has been achieved [2, p.576-593]. The increase in conductivity is directly proportional to the dopant concentration, thus if a conductive network is present, the amount of valence electrons restricts the conductivity.

2.2 Conductive filled polymers

Polymeric solids with conductive particles dispersed into the matrix are able to conduct electricity via phenomenon called percolation, in which the charge is transported along a network formed by filler particles. Due to isolating behaviour of the polymer, the concentration of conducting fillers has to be higher than percolation threshold. As the threshold is exceeded a transition from insulator to conductor occurs. The particles do not necessarily have to form a physical contact between each other, instead a small layer of polymer can exist in between of conducting particles. This is owing to the quantum tunnelling of electrons. Quantum leaps of over 2–5 nm have been observed in various reports [5, p.172–173].

Conductivity above the percolation threshold can be estimated according to Tunnicliffe *et al.* in a binary system with the following equation:

$$\sigma = \sigma_0 \frac{\Phi - \Phi_c{}^{\mu}}{1 - \Phi_c} \tag{2.3}$$

where σ is the DC conductivity, σ_0 is the DC conductivity above percolation threshold, Φ is the volume fraction of filler loading, Φ_c is the volume fraction at percolation threshold and μ is the power law exponent [6].

To describe the percolation curves and their behavior, carbon black and short carbon fiber in matrices of ethyl vinyl acetate (EVA) and natural rubber (NR) are represented in **figure** 2.2 according to the results obtained by Das *et al.* [7]. The conductive behaviour changes remarkably depending on the used filler-matrix combination.

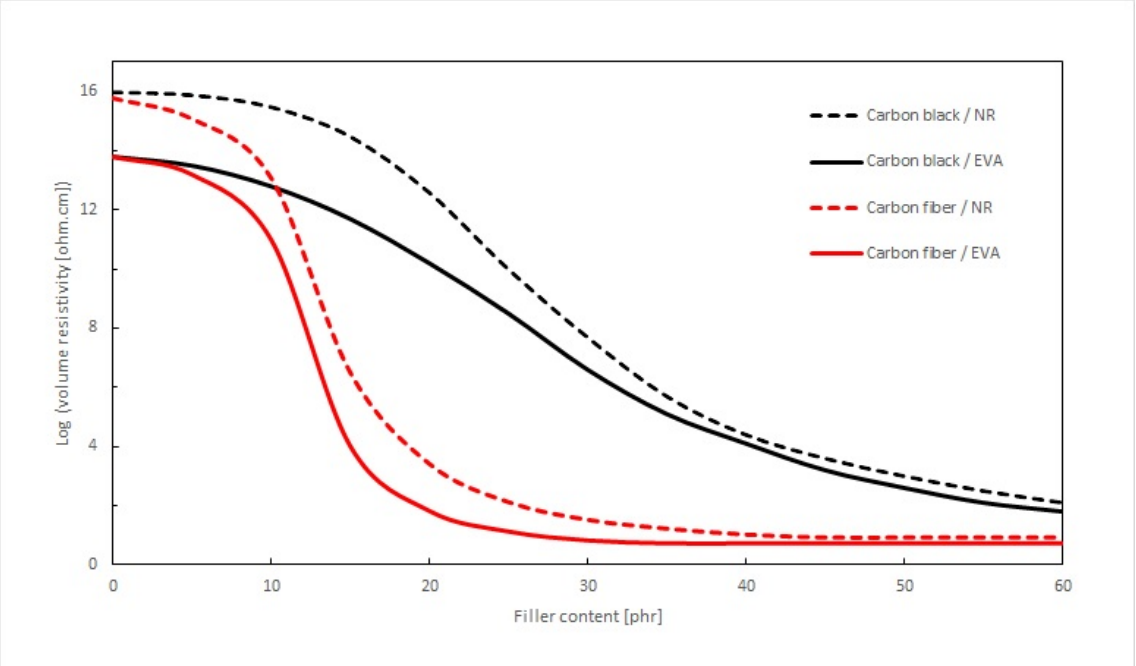

Figure 2.2 *Percolation curves for conductive carbon black (Vulcan XC 72) and short carbon fiber in EVA and NR matrices. Redrawn from [7].*

As seen from above, (volume) resistivity exhibits a very non-linear behaviour near the threshold concentrations. It is typical that the resistivity sets to a certain level, after which a further increase in filler content ceases to affect the conductivity considerably. The intrinsic conductivity of a filler represents the upper limit for the filled material. The source of difference in conductivity between the filler and its composite resides in the conductive network and its formation [5, p.175–176]. Since conductivity is affected by variables such as filler geometry, constitution and

surrounding matrix, multiple approaches can be used for tailoring the electrical properties of a polymer composite. These areas will be viewed in more detail in the following chapters.

2.3 Percolation and its modelling

Percolation is a general phenomenon in which a dispersed component forms an interaction path within a heterogeneous system. Percolation modelling is based on mathematical expressions, where the probability of occurrence is studied. This thesis addresses only the electrical percolation of conductive fillers.

The general assumption in percolation modelling of filled polymers is, that electrons and heat are able to transfer efficiently only when the filler particles are in contact with each other. The aforementioned quantum tunnelling makes the network formation easier, thus the conductivity in a real scenario is likely better than the model's, if the inter-particular area is not taken into account. The formation of particle network is affected by the dimensions and geometry of the particles. In order to establish a connection between the particle concentrations and the values of conductivity, experimental data is required.

Two widely accepted models are used in the estimation of percolation threshold, the first of which is named the average bond number method. It is based on calculating B_c, the amount of particles that contact a single particle of interest. This method yet lacks in its theoretical basis and since B_c is material dependent, it cannot be used for estimation without the support of experimental values. [8]

The second one is the excluded volume model, in which a particle defines a volume where the centers of similar particles are not permitted to exist. Since the orientation of particles varies, the excluded volume of a particle is defined as an average excluded volume $\langle V \rangle$. The total excluded volume $\langle V_{ex} \rangle$ is given by multiplying the average excluded volume of a single filler with the critical concentration N_C of a filler, that is equivalent to percolation threshold i.e. the smallest concentration required for charge transfer throughout the material volume. The average bond number and excluded volume are conceptually similar quantities in the case of permeable particles in continuum: Since B_c is the average number of particle contacts per given particle, it is also the amount of particle centers, that enter the excluded volume of a given particle. This dependency can be written as

$$B_c = \langle V \rangle N_c \equiv \langle V_{ex} \rangle \tag{2.4}$$

Depending on the studied system, whether it is a lattice or continuum and if the spheres have hard or soft core, the values for B_c are more affected by changes than $\langle V_{ex} \rangle$ values, thus excluded volume model can be considered as the more universal concept on behalf of invariance [9].

For a given filler depending on its geometry, there is a proportionality factor **k**, which connects the amount of particles per unit volume V_{unit} to the average excluded volume of a particle, this inverse proportional relationship [10] can be expressed as

$$N_c = k \frac{V_{unit}}{\langle V \rangle} \tag{2.5}$$

According to the equation 2.5 each V_{unit} can be thought to consist of N_c smaller volumes. The size of a small volume is $\langle V \rangle / k$. The percolation occurs, when all the small volumes are occupied and as a result the average excluded volume in a volume unit is constant at the threshold. These previous equations are usable only with systems, that contain only single type of a filler with narrow size distribution [8].

2.4 Modeling of percolation in hybrid filler systems

It is possible to use more than single type of a filler inside the matrix - such compounds are called hybrid filler systems. The term hybrid refers to a mixed composition, which in this case is equal to having more than one reinforcing or filling material in the system. In contrast, hybrid materials can also consist of multiple matrices and by definition they are ought to exhibit superior properties or functions, which cannot be attained with the single components. The rule of mixture does not apply for hybrid materials or nanocomposites, since the interfacial filler-matrix adhesion or interaction between the fillers is not considered. [11]

The small volume concept is schematically represented in **figure 2.3** for CB and CNT geometries in ternary systems. It should be noticed that **figure 2.3a** is a simplified presentation of the dispersed state, in which the different excluded volumes of fillers are not applied.

Sun *et al.* have studied ternary combinations of CB, graphite and CNT. They observed that the percolation threshold of a ternary system is always in between of the thresholds obtained in separate binary systems. Based on these results they developed a simple model, which aims to take the different filler shapes and excluded volumes into account[10]. The model assumes a linear relationship between fillers A and B. Percolation in hybrid filler system occurs when

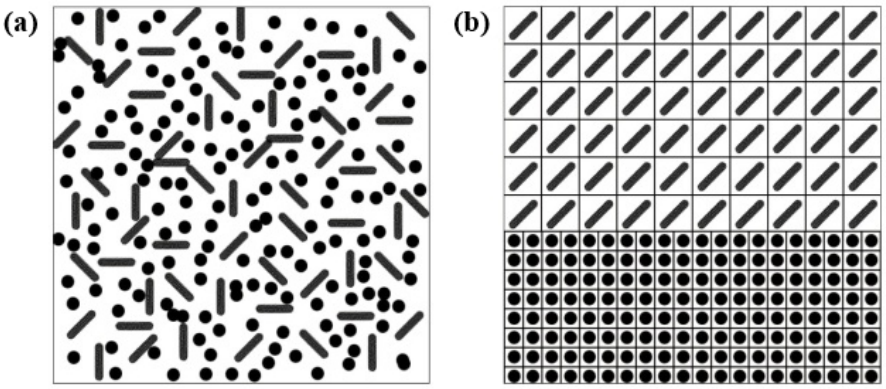

Figure 2.3 *Schematic presentation CNT+CB hybrid filler system in a) dispersed state b) non-mixed state. Modified from [10].*

$$\frac{m_A}{P_{c,A}} + \frac{m_B}{P_{c,B}} = 1 \tag{2.6}$$

where the weight fractions are m_A and m_B and percolation thresholds in binary systems are $P_{c,A}$ and $P_{c,B}$, respectively.

The prior equation does not take into account the synergistic effect between different fillers since the degree of mixing is not reviewed. If percolation is observed and the prior equation results in a value, that is lower than 1, then a synergistic behaviour is ought to exist. Chen *et al.* continued the Balberg's concept of excluded volume by modifying the average intersection number to describe the behaviour in hybrid filled polymer composites [8]. Their equation considers particles that are spherocylindrical, e.g. CNT, and spherical, e.g. carbon black, in the following form of

$$\frac{\Phi_i^2}{\Phi_i^{th}} + \frac{\alpha^2}{\lambda}\frac{\Phi_i\Phi_j}{\Phi_j^{th}} + \frac{2\alpha^3}{3\lambda}\frac{\Phi_j^2}{\Phi_j^{th}} = \Phi_i + \frac{2\alpha^3}{3\lambda}\Phi_j \tag{2.7}$$

where Φ_i, Φ_j are the filler volume fractions and Φ_i^{th}, Φ_j^{th} are the percolation thresholds in binary systems for spherical and cylindrical particles, respectively. α is the ratio of filler diameters d_i/d_j and λ is the aspect ratio of the cylindrical filler. In this equation $l_j >> d_i >> d_j$ is assumed and should be taken into consideration if other type of fillers are to be modelled. **Eq.** 2.7 is plotted in **figure** 2.4 against the results obtained from Monte Carlo simulations and the volumetric version of **eq.** 2.6 [8].

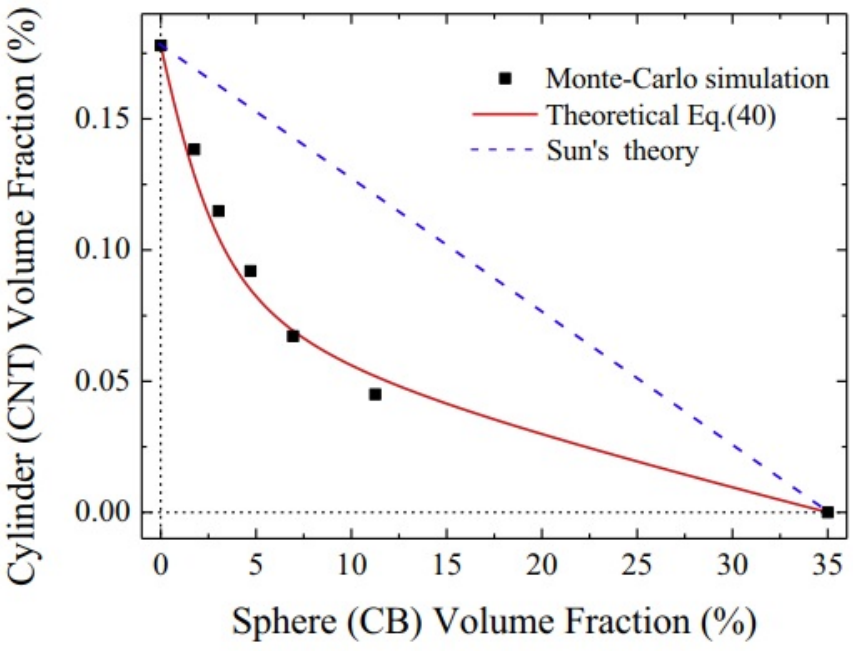

Figure 2.4 *A comparison of Monte Carlo simulations and percolation models of Sun et al. and Chen et al. [8]*

As it can be seen from **figure** 2.4, the Monte-Carlo simulations and **eq.** 2.7 suggest that the effect of synergism is remarkable. This type of behaviour however requires high degree of dispersion from every constituent of the system, thus in melt processing applications **eq.** 2.6 might offer an adequate solution for designing, if the system parameters or assumptions prevent the use of **eq.** 2.7.

3. THE EFFECT OF MATRIX MORPHOLOGY ON CONDUCTIVITY

The dispersion state of a filler inside a polymer depends on factors such as the melt viscosity and surface free energy of the polymer, and the size of the filler particles. In the case of having an incompatible polymer blend with components that have similar viscosities, the distribution of filler particles is mainly decided by its affinity to each component[12]. If the matrix blend consists of two rheologically very dissimilar matrices, the filler distribution is selective towards the polymer where its flow is less restrained, which is typically the one with lower viscosity.

3.1 Phases and interfaces

Surface tension γ, or surface energy, is an essential material property in order to assess the behaviour of heterogeneous components in a dispersion. The former is force per unit length while the latter is force per unit area. They are both describing the force that drives to minimize the area of an interface, which is illustrated in **figure** 3.1 for atoms near a liquid-gas interface. Within a solid material the average attractive forces experienced by a single atom over time are isotropic, whereas at the interface the lack of adjacent atoms in gaseous phase results in a net force away from the interface. As a consequence of being under tension, water droplets are spherical in air, but tend to expand over substrates exhibiting higher surface tension - this is also known as wetting [13, p. 10–13].

The tendency of a polymer to wet filler particles in conductive blends contributes to multiple factors, e.g. the stress distribution from matrix to particles, dispersion quality and formation of particle networks. These features define a major portion of materials' performance, thus the interfaces can be regarded as a matter of importance.

The formation of conductive networks in the interphase area is dependent on the interfacial energy of the matrix and fillers. If a material has high matrix/filler interfacial energy, the filler-filler interactions are energetically favored, thus conduc-

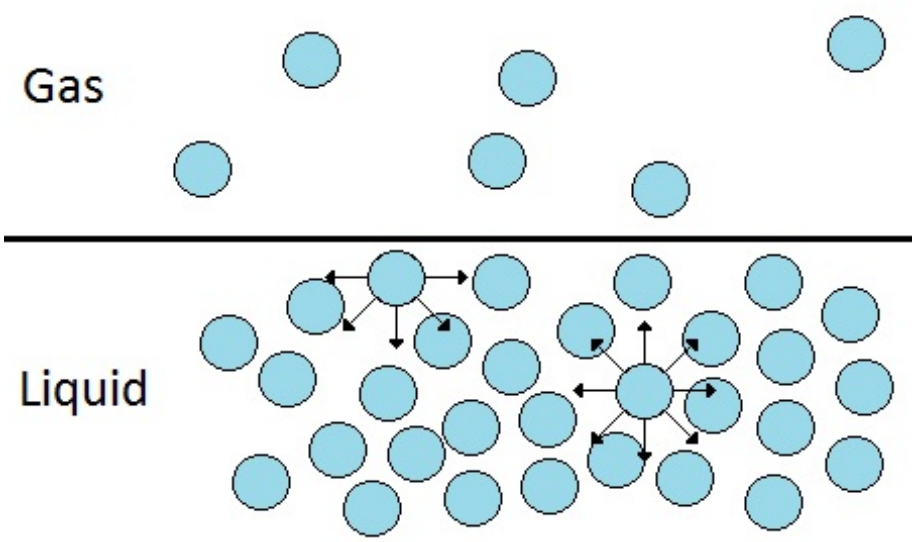

Figure 3.1 *Schematic presentation of how the inter-atomic distance affects on the attractive forces near a liquid-gas interface. Redrawn from [13, p. 12].*

tive networks are prone to form [14]. Sumita *et al.* have introduced a qualitative equation[12] that predicts the distribution of CB by calculating a wetting coefficient as followed:

$$\omega_{A-B} = \frac{\gamma_{CB-B} - \gamma_{CB-A}}{\gamma_{A-B}} \tag{3.1}$$

where γ_{CB-A} and γ_{CB-B} are the interfacial free energies between the matrices and the filler, and γ_{A-B} is the interfacial energy between the matrices. According to the resulting wetting coefficient, the preferred location of CB is follows the next principles:

$\omega_{A-B} < -1$	Matrix A
-1 $< \omega_{A-B} <$ 1	Interface
$\omega_{A-B} > 1$	Matrix B

Utilization of interfaces in the formation of conductive blends has been widely studied. In general, complex blend morphologies and selective localization of particles in the polymer phases or phase boundaries are methods that have been successfully used in many reports [14] [15] [16] [17].

Equation 3.1 does not apply in situations, where kinetic and processing factors

are stronger. Kinetic factor is defined by the viscosity difference between present matrices while the processing factors include the distribution caused by processing sequence and mixing conditions. For PMMA/PP blends it has been found that by using a PMMA grade that has similar viscosity than PP the carbon black particles reside in PMMA phase - as predicted with the former equation. However, when PMMA is changed to more viscous grades, the preferred location is shifted to the interface and finally to the PP phase [16].

Zhanga *et al.* have experimented the conductivity of vapour grown carbon fibers (VPCF) in a HDPE/i-PP matrix. The achieved percolation threshold was only 1.25 phr and from the SEM micrographs, it was observed that the fibers were selectively located in the HDPE-phase. In their study, the specimen were compression molded from a two roll milled batch. The resulting percolation curves for both matrices alone and their 1:1 blend are illustrated in **figure** 3.2. For efficient usage of blend interfaces, so called double percolation has to occur: First the percolation path should be achieved inside the HDPE-phase and then the HDPE-phase should form a continuous phase within the material. [14]

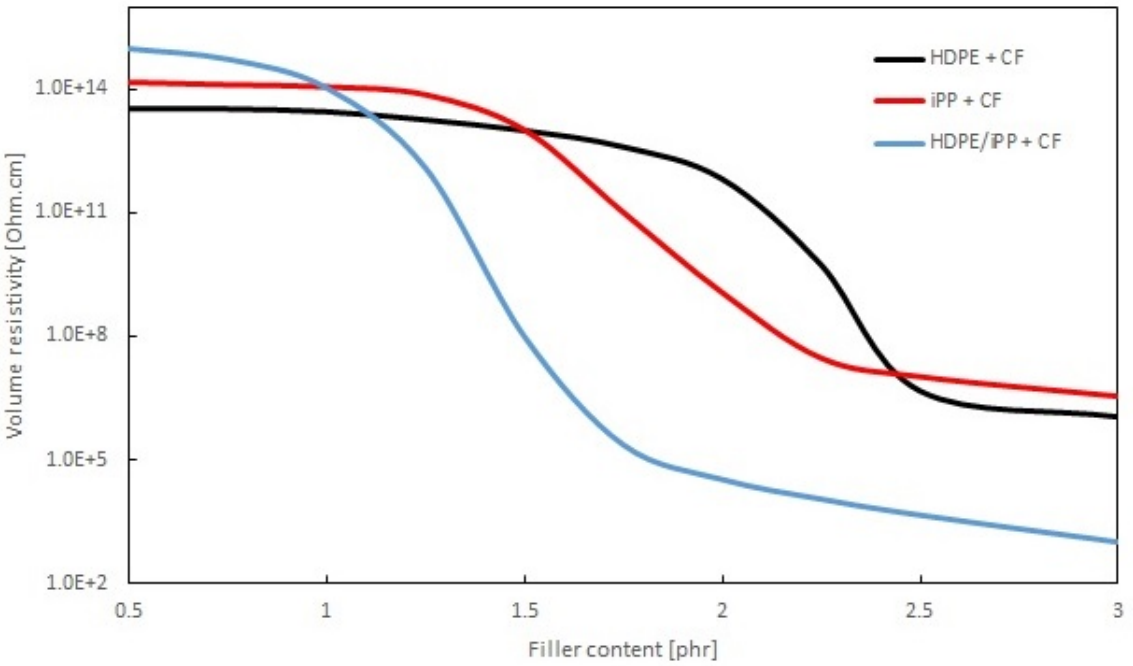

***Figure** 3.2 Polymeric blends can form co-continuous morphologies, where the achieved electrical performance is more efficient when compared to the polymer matrices alone as shown above for high density PE and isotactic PP. The figure is redrawn according to [14].*

In compounds of multiple polymer matrices, filler particles are more easily dispersed into materials with lower surface energy γ, thus in HDPE/PP blends with $\gamma_{HDPE/CB}$ = 2.2 mJ/m^2 is preferred over PP with $\gamma_{PP/CB}$ = 4.1 mJ/m^2. Shen *et al.* have ve-

rified this type of behaviour with SEM-imaging in hybrid filled systems with different combinations of HDPE, PP, CB and CF. The selective location of CB in the HDPE-phase and the double percolation behaviour are easily seen in **figure** 3.3.

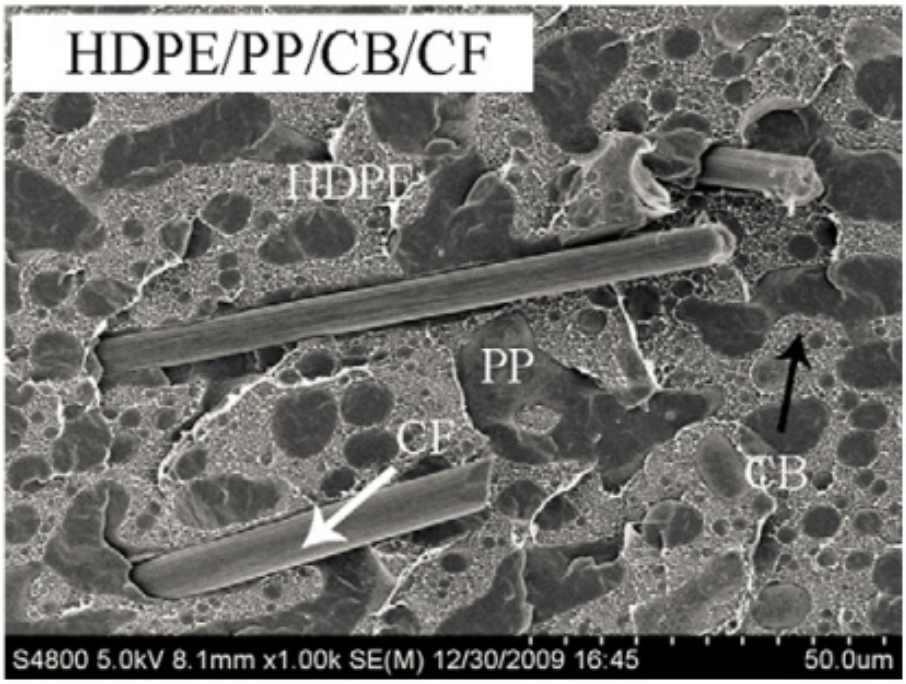

***Figure** 3.3 A SEM micrograph of CF+CB filled HDPE/PP blend, where the preferential location of carbon black in HDPE can be seen along with the well segregated polymeric phases. Edited from source [15].*

The 2-dimensional illustration of different co-continuous phases is shown in **figure** 3.4. From figures 3.3 and 3.4 it can be clearly seen that the schematic presentation depicts the reality in this case.

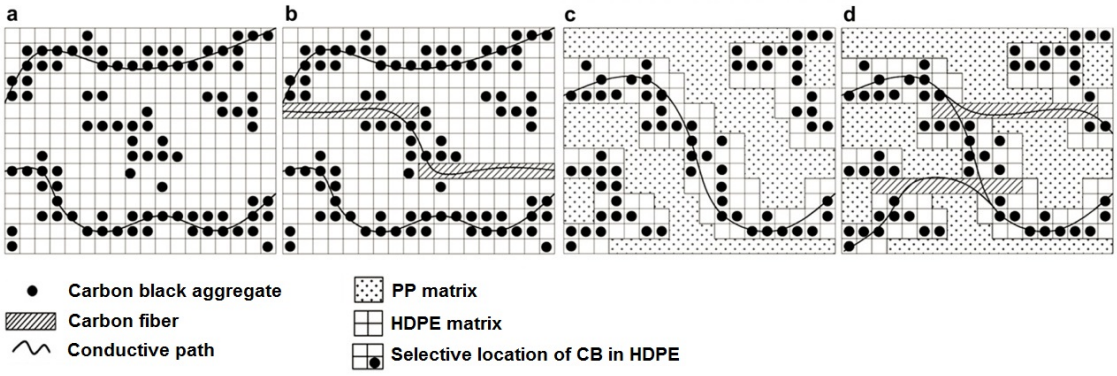

***Figure** 3.4 Microstructure and conductive networks schematically presented in (a) HDPE/CB; (b) HDPE/CB+CF; (c) HDPE/PP/CB; (d) HDPE/PP/CB+CF composites with CB concentration above percolation threshold in HDPE matrix. [15]*

As seen from the previous figures, CB particles tend to form most of the dispersed conductive network while CFs provide longer unobstructed pathways for charge transportation. CFs are distributed into both phases including the PP-phase, which contains only a little amount of CB particles, thus the probability of double percolation is increased. The CB agglomerates provide better connectivity between carbon fibres by increasing the conductive surface area near individual carbon fibres.

Immiscibility in polymer blends has been shown to affect to the electrical properties in multiple ways. For CB the affinity is typically stronger for the polymer, that has a higher percolation threshold in a binary compound, which is often the polymer with higher surface tension. The resistivity is affected by the blend morphology and the location of CB. Breuer *et al.* have studied CB filled blends of HIPS/LLDPE. Polymer blends were noticed to exhibit lower percolation thresholds in general when compared to binary systems, but behave very differently when the polymer ratios and filler concentrations are changed. The lower the filler concentration is, the more conductivity depends on the blend ratio and formation of co-continuous structures. Their results also indicate that surface tension, viscosity ratio of the polymers and the level of shear stress affects to the final morphology of immiscible blends [17].

3.2 Crystallinity

Polymers differ from other material classes in multiple aspects, one of which is that they do not exist in strictly ordered structures. Instead the temperature of a polymer defines whether it is a solid, a low viscosity melt or something from between. For some polymers, i.e. semicrystalline, the shift from solid to melt occurs in a narrow region, which is known as the melting temperature of a polymer. The polymer molecules are driven towards a minimum energy state, which results in crystallinity. Polymers that do not exhibit crystallization are called amorphous. As a physical phenomenon, crystallinity is complex to define since the shape of a crystallite varies depending on the structure of a polymer. Spherulitic crystal growth, i.e. growth in the radial direction away from the nucleation center, is typical for many common polymers [18, p. 382]. Incorporation of fillers alters the situation as increased amount of nucleation sites causes trans-crystallinity - when crystals nucleate nearby, they are forced to align in certain directions instead of growing radially. As a result trans-crystalline layers with typical thickness of 10–30 μm are formed, of which even the whole matrix can consist of.

While studying the effect of graphite particle size (see **section** 4.3), Nagata *et al.* came to a conclusion that the particle size affects to the crystallization kinetics. The crystallite size and degree of crystallinity of LDPE-matrix were measured along the

rolled plane and across the thickness. In the cross-sectional measurements a slight increase of crystallite size could be seen as a function of filler content. Along the rolled plane a non-linear increase was observed for the particle sizes of 14.5 μm and below, which was clearly higher than with particle sizes of 25.7 μm and above. The main cause was interpreted to be the ease of alignment for small particles. In the degree of crystallinity a more sudden increase with the lower concentrations of graphite was observed for the smaller particle sizes - the overall trend was that crystallinity increases as concentration increases in the plane of orientation, while it remains nearly invariant, approximately 40%, in the cross sectional samples. [19]

Below the melting temperature of a semi-crystalline polymer the matrix contains dense crystalline regions, that are hard to permeate for filler particles. The local concentration of conductive fillers in the amorphous region is increased as the degree of crystallinity increases, thus the percolation threshold can be expected to be lower. The coefficients of thermal expansion of polymeric matrices are often higher than the fillers', which typically translates to resistivity increasing along with the temperature. In amorphous polymers the expansion takes place in the whole component, while in semicrystalline polymers the crystallites are nearly unaffected under the melting temperature. The fillers preferentially exist in the amorphous part of the matrix. For semicrystalline materials the amorphous regions have higher local concentrations of filler particles, which makes them less affected by temperature changes under the polymers' melting temperatures.

At the melting temperature of crystalline polymer, the total volume of the system is increased significantly and the local filler concentrations are diluted, which in typical cases for the semi-crystalline polymers can be seen as a peak in resistivity. This phenomenon leads further to positive and negative temperature coefficient effects, denoted with PTC and NTC. In the latter, the resistivity drops suddenly when measurement temperature is above the melting temperature, which is due to increased mobility and formation of flocculated structures. This kind of behaviour is typical for semicrystalline CB-filled polymers. In PTC effect, the resistivity stays at an elevated level above the melting temperature.

Feng *et al.* studied ultra high molecular weight poly(ethylene) in PP/UHMWPE blends and their negative and positive temperature coefficients. They managed to eliminate the NTC effect by varying the ratio of PP/UHMWPE in their blend while keeping the filler content constant [20]. According to their results the resistivity in room temperature and above can be tailored by changing the weight ratio of the polymer components, CB content and the CB particle size. One of the most important reasons behind these observations was the very high viscosity and crystallinity

of the UHMWPE, which was shown to have a repulsive affinity for carbon black. On top of achieving a PTC effect with their blend formulations, they found a way to control the resistivity at high temperature by using different grades of carbon blacks together in various ratios.

Pötschke *et al.* found in their studies of composites containing both CNTs and carbon black, that including either of the nanofillers would increase the melting and crystallization temperatures by several degrees [21]. However, the results seemed to be invariant of the type and concentration of the filler, and synergistic effects were not seen when both fillers were incorporated. Thus the crystallization was concluded to be unaffected by incorporation of a second filler.

3.3 Compatibilization

The polymer phases are often dissimilar, e.g. polar and non-polar homopolymer, which are not able to adhere well with each other due to interfacial tension. It will lead to poor mechanical behaviour if compatibilizing substances are not incorporated. These substances are mainly block- and graft copolymers, which are microphase separated into domains that are similar to the main phases in the blend. A common feature of block-copolymers in immiscible blends is their migration to the interfaces, where they penetrate into the adjacent phases, thus increasing the interfacial area and lowering the surface tension. The effectiveness of the compatibilizer correlates with the occupied interfacial area, thus higher concentration of copolymer leads to more uniform blend morphology. The degree of miscibility determines the tendency of compatibilizing molecules to localize, and after a certain concentration the interface becomes "crowded"and promotes the formation of micelles. [22, p. 412–419]

As mentioned in the earlier sections, the interfacial tension and phase boundaries provide a possible mechanism for achieving lower percolation thresholds. Thus, the addition of a compatibilizing third component can result in less pronounced phase boundaries. While it might be a route to achieving good conductivity, it is often not the case, that it should be pursued without considering the decrease in mechanical performance. Possible solutions could be either finding a ratio of polymers, that is adequate yet leaves some interfaces intact, or by incorporating fillers with low affinity for certain phases. More of the latter is reviewed in **section** 4.5

4. CONDUCTIVE CARBON FILLERS

The element carbon has a large amount of allotropes such as graphite, carbon black, fullerene, and diamond. Even though diamond exhibits some of the best properties known, its conductivity is low due to completely bonded chemical structure. As in the case of ICPs, carbon relies on structures that are based on conjugated double bonds. The hexagonal basal structure of graphene is shown in **figure** 4.1.

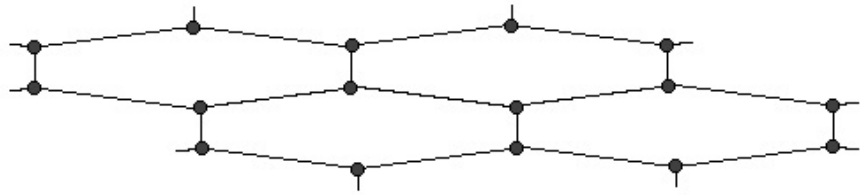

Figure 4.1 *Schematic presentation of graphene's chemical structure.*

By twisting the structure into tubular shape, it represents the structure of a carbon nanotube. By stacking graphene sheets, graphite is attained. The structure, size and form of bonding defines the filler's performance. In general, the more homogeneous the structure is, the better intrinsic properties it has. The effect of bonding can be seen when the properties of graphite and graphene are compared. Despite graphene being among the strongest materials known, graphite is a poor reinforcement, which is due to the weak inter-planar bonding. The latter is much easier to produce and process, and comes with a lower price tag, thus choosing the right carbon allotrope depends a lot on the wanted outcome.

The role of a conductive filler is to introduce electrical properties to the system, while minimizing its negative effects. One typical unwanted side effect is brittleness, which is mainly caused by weak particle-particle bonding - above percolation threshold particles form continuous paths throughout the material, which often results in deterioration of mechanical properties. An increase in filler size and concentration is also known to affect negatively to the mechanical performance of a composite [23, p. 306–308].

The basis for tailoring the electrical properties of a polymeric solid lies in the formation of particle network. Particulate fillers like carbon blacks should form dendritic structures for efficient charge transportation [5, p.175–176]. These structures often consist of finite sized aggregates, i.e. particles that are adhered to form clusters due to inter-particular forces. [23, p. 359–360]. The relationship between carbon black's structure and main characteristics are visualised in **figure** 4.2.

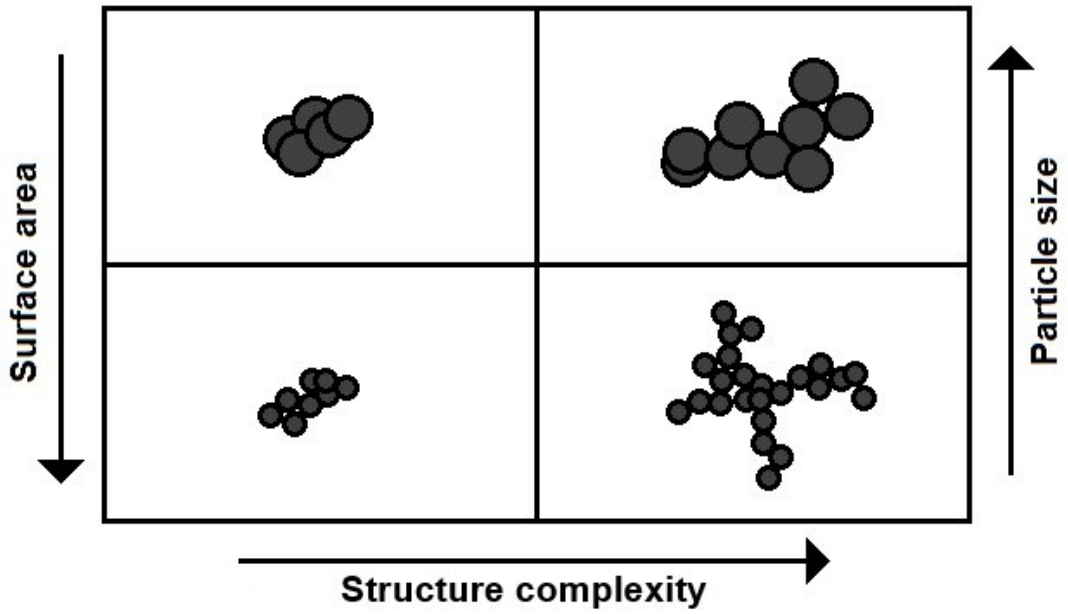

Figure 4.2 *The structure-property relationship of carbon black aggregates. Redrawn according to [24].*

Dispersion and dispersion quality are terms, which assess the spatial arrangement of particles within the composite. Characteristics for good dispersion are small primary particles homogeneously located throughout the material. This can be achieved when the polymer melt undergoes distributive and dispersive mixing. Dispersive mixing can be detrimental to the conductivity after a certain point has been exceeded due to breakage of filler structure and decreasing size of agglomerates. For fillers with high aspect ratio, random isotropic distribution is preferred over aggregated structures. On the other side larger aspect ratio makes it easier to form anisotropic structures if such properties are desired.

In **figure** 4.3 different factors that affect to the dispersion of a filler are presented. The main effects related to the operating conditions and wetting were briefly gone through in chapters 1 and 3, while the next sections address the issues related to the fillers.

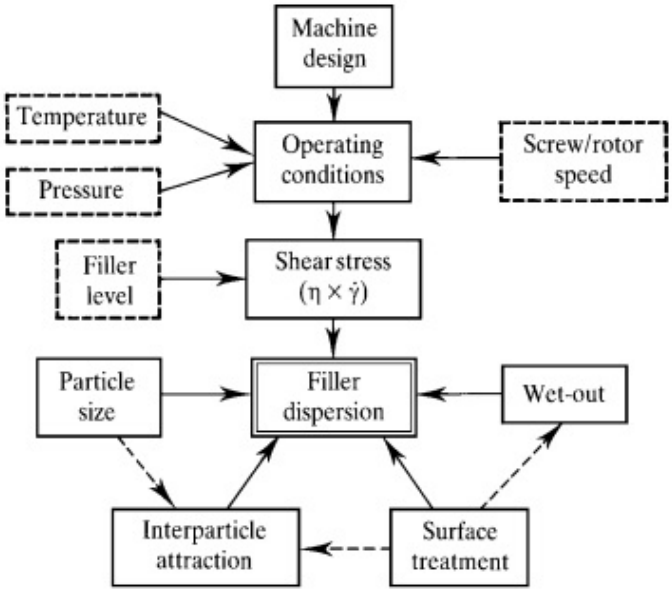

***Figure** 4.3 Factors, which contribute to the formation of dispersion quality [18, p. 216].*

4.1 Particle-particle interactions

The potential energy of two adjacent particles is a trade-off between attractive London-van der Waals forces and repulsive Coulombic forces. The latter forces form a barrier between two minimum energy states, which has to be overcome if separate particles are wished to agglomerate. The shift over the barrier can be achieved by decreasing the inter-particular distance with shear mixing or by increasing the ionic concentration to enhance the attractive forces. The tendency of agglomeration depends also on the particle geometry and constitution. Within a particle there can be accumulation of positive and negative charge in different areas, which contribute to the formation of filler-filler networks. [23, p. 318–319]

Agglomeration and flocculation are two similar phenomena, in which primary particles form bigger structural units - the difference is that agglomeration is used to describe particles in their solid state, while in flocculation a liquid medium is present. Following forces promote adhesion between particles according to [23, p. 320]:

- **Bridging forces:** sintering, melting, the effect binders, chemical reaction
- **Adhesion and cohesion forces:** the effect of viscous binders and absorption layers
- **Attraction forces:** van der Waals, hydrogen bonding, electrostatic and magnetic
- **Interfacial forces:** liquid bridges (H_2O-Hydrogen bonding), capillary.

The tendency of particles to agglomerate depends on multiple factors such as the type of bonding, particle size, surface chemistry, type of surface, surface treatments and moisture level. The agglomerates in carbon blacks consist of aggregates - the attractive forces within the aggregates are typically strong enough to resist breakup during mixing and grinding. Aggregates can be characterized with 3 quantities: the size of primary particles, number of primary particles and their structural configuration within the aggregate. Carbon blacks are categorized as low and high structure CBs. The former are spherical with limited branching while the latter are grape-like with high degree of branching. The particle-particle and particle-matrix interactions are easier to form with structural CBs since they are more stable. The low structure CBs have more degrees of freedom and are able to re-agglomerate easily within a polymer melt. [23, p. 321]

Agglomerates can be broken down to aggregates under shearing conditions for better dispersability. The agglomerated structures can also be re-formed when adjacent particles coalesce. The magnitude and rate of flocculation has been observed to be related to the surface free energy (SFE) of carbon black particles. Tunnicliffe *et al.* suggested that the significant decrease in percolation threshold was caused by reduction of SFE. The graphitization was deduced to decrease the effective viscosity by weakening the bonding between the matrix and filler particles, which is consistent with their results of modified fillers exhibiting more fragile behaviour. The tested carbon black types were N134, N330 and N990. Such behaviour was not observed in N990, which has the largest particle size and lowest structure. [6]

4.2 Particle shape and aspect ratio

The shape of a particle can provide various advantages, of which a list is given below according to [23, p. 313]. Aspect ratio λ is used to describe a particle's dimensionality. It is calculated by dividing the length of the particle with its diameter, i.e. for a perfect sphere the aspect ratio is 1.

Table 4.1 *Examples of particle shapes and their advantages*

Shape	**Features**
Spherical	High packing density, low viscosity, uniform distribution of stress, increased flow in melts and powders
Dendritic	Large specific surface area
Tubular	Excellent reinforcement, reduction in shrinkage and thermal expansion, promotes thixotropic properties
Flake	Low permeability of liquids, gases and vapors, facilitates orientation, large reflecting surfaces
Irregular	Easy to produce, inexpensive

High intrinsic conductivity of a particle combined with high aspect ratio is known to lead to low percolation threshold values [23, p. 359–360]. According to a suggestion based on the excluded volume model a following relationship exists between aspect ratio and percolation threshold [25].

$$\Phi_c \approx \frac{1}{\lambda} \tag{4.1}$$

This equation is at best an approximation, since fillers are far from ideal particles and exhibit different kind of properties. However, it can give a rough estimation of the filler's potential performance in conductive applications.

For CNTs even low concentrations of 1-3% can provide good conductivity. To get a similar results with particles of lower aspect ratio, the concentrations are typically 10-20 times higher. [3] Percolation thresholds of 0.9 wt-% and 1.5 wt-% have been observed for carbon nanofibers (CNF) and multi-walled carbon nanotubes (MWCNT) dispersed in PSF, with the aspect ratios of 500-2000 and 10-800, respectively [23, p. 359–360]. Even though these values are very low, they are still far from the predictions with **equation** 4.1. The differences probably have multiple causes with the poor dispersion quality being the governing one.

The aspect ratio has been shown to affect the electrical behaviour in LDPE/graphite composites. A spherical particle with the size of 5.1 μm was compared to multiple flake-like particles with aspect ratio of 10-15 and size 2.1-82.6 μm. The lowest conductivity was obtained with the spherical particle, and since the composition is similar, the effect of aspect ratio on conductivity dictates over the filler size effect. [19]

4.3 Filler size and size distribution

The size of a filler together with its geometry defines its specific surface area, which is a remarkable factor in defining how efficiently the filler can form a network within the composite. Since the filler-filler interactions act at the interfaces, also the reactivity of the filler is increased upon decrease in size.

The gravitational force is proportional to the mass of an object. As the filler size decreases, the effective electrostatic forces grow stronger and affect more to the behaviour of the filler. Smaller particle size equals to greater surface area, which can be seen as an increase in the amount of van der Waals forces, interaction points and surface groups. Thus the reactivity of the filler is higher for small particles. Since the dispersed particles are able to interact more with the polymer, the material is harder to process, which leads to an increase in viscosity. The following studies conform this kind of an effect of particle size to the degree of dispersion [19] and to the filler-matrix interactions [26] without contradicting even though the fillers and matrices are very dissimilar.

Nagata *et al.* studied the effect of filler size on the conductivity of a graphite filled LDPE composite. The mixture was made by hot rolling, after which it was compressed into sheet form and quenched. Their studies included graphites with sizes: 2.1 $\mu m, 5.8\ \mu m, 14.5\ \mu m, 25.7\ \mu m, 50.8\ \mu m, 82.6\ \mu m, 5.1\ \mu m$. The main geometry of the six first is flake-like, and the last one is spherical. Small filler size was seen to contribute to the formation of crystalline areas of LDPE at the graphite surfaces, and their X-ray diffraction results indicate that small particle size leads to a close-packed filler structure. As a consequence, the percolation threshold was observed to increase linearly as a function of graphite size with the spherical graphite as an exception, due to its lower aspect ratio. [19]

Kim *et al.* have confirmed similar kind of dependency on conductivity with silver flakes dispersed in epoxy. Their studies included four specimen (A,B,C,D), where the fourth was a mixture of samples A and C in the ratio of 1 to 13,63. The lengths of samples A-C were 3.2 $\mu m, 7.6\ \mu m$ and 9.9 μm and the thicknesses were 0.4 $\mu m, 0.8\ \mu m$ and 1.0 μm, respectively. The samples B and D had roughly similar average size, but the latter had a broader size distribution. The conductive behaviour of sample D was enhanced by the addition of smaller particles. Their main conclusion was that the surface to volume ratio is an important aspect, which affects to the electrical conduction by affecting to the fillers' interactions with the polymer matrix. The ratio is dependent of the filler shape, size and size distribution. [26]

4.4 Surface chemistry

The flow of charge in a composite depends on the conductive network and its composition. In carbon-based fillers the charge transportation occurs through the graphitic basal planes. The most important factor that restricts the flow of charge within a carbon black filled system are the interfaces between carbon black aggregates [27]. The chemical bonding at the the carbon black aggregates' surfaces binds the electrons and increases the distance between conductive structures. Carbon blacks are mostly nonpolar despite the chemical groups existing on their surface, for which reason they are compatible with nonpolar polymers.

The surface chemistry and morphology of a filler is a product of used manufacturing method, processing conditions and other treatments. The exact structure of carbon black is not well known, and it is thought that the surface groups are located on the edges of graphitic surfaces. The surface groups can originate from chemical treatments or they can be products of oxidation. The surface groups that are mutually agreed to exist in carbon black structure are carbonyl and hydroxyl group [23, p. 376]. The existence of carboxyl and lactone groups or sites of unsaturation is less mutual. Furnace and thermal blacks contain higher amounts of impurities, i.e. not carbon, than conductive blacks. The latter are produced in higher temperatures where chemical groups containing elements such as sulphur or oxygen are removed from the structure. The conductivity of a carbon black has been found to correlate with the *graphitic character* of the surface, which describes how comparable the structure is to a perfect graphite layer [27]. Elemental analysis alone does not provide enough information, as some grades of carbon blacks contain small amounts of impurities yet are more conductive than CBs consisting of carbon only, thus other methods, e.g. XPS, that provide more information about the surface are required.

Breuer *et al.* have noticed in their studies that the slightly polar and basic nature of PS allows acidic interactions with the surface of carbon black. When compared to segregated structures of PE or PP, HIPS is more prone to form uniform particle distributions. [17]

4.5 Hybrid filler systems and synergism

The use of multiple different particles can result in a remarkable change in the final properties and broadens the possibilities in property tailoring. In this section multiple studies, where different utilizations of hybrid fillers have positively influenced the materials' behaviour. Some of the synergistic behaviours are explained with models.

Lu *et al.* have studied the different ratios of CB to CF in hybrid filler systems and found that CF content can be partially substituted with a cheaper and less conductive CB with only slight changes in conductivity. According to their experiments, if the initial amount of CF is over 10 wt-% up to 5 wt-% can be replaced with CB, if it is lower than 10 wt-% the amount of replacing CB should be less than 2 wt-%. The conductivity value is shown to depend greatly on the CF content, but is also affected by further addition of carbon black. The relative conductivity increment is shown to decrease as the CB content increases. Lu *et al.* accomplished to get similar conductivities with samples that were, prior to hotpressing, mixed either in dissolved or melted state. The ratio of CB to CF was altered from 1:1 to 1:3 providing transient results between the behaviors of the binary systems. [28] Similar conclusion was made by Sumfleth *et al.* A significant portion of CNT content can be replaced with other conductive filler, e.g. carbon black, if it possesses similar kind of re-agglomeration properties [29].

A study of CB+CF hybrid filler in polypropylene matrix has been conducted by Drubetski *et al.* with the focus on achieving synergistic behaviour in injection moulded samples. Their results also indicate synergism between the fillers, even though they used a highly structured CB unlike Lu *et al.*. To complement the analysis based on resistance measurements, other indicators of synergism including morphological analysis and fiber length measurements were carried out. They came to two conclusions, first of which is that the presence of carbon black particles accelerates the fiber breakage, and the second is that carbon black particles inhibit the flow induced fiber orientation during injection moulding. Confirming tests with glass fiber were made, which showed that the latter phenomenon is not specific for CFs. The fiber orientation was further studied in two PP matrices of different viscosities and it was noticed that the higher viscosity leads to higher volume resistivity, higher percolation threshold and enhanced fiber orientation. The fibers preferred perpendicular alignment to the flow with both matrices, thus the presence of carbon black inhibits flow orientation more than the viscosity promotes [30].

It has been studied that in CB+CF hybrids the particles tend to form something called "grape-cluster-like"structures, where carbon black particles gather in the vicinity of the carbon fiber enhancing the conducting surface area near CFs. However, due to the relatively low aspect ratio (≈ 100) of CFs, the effectivity of CF is rather small. Also the straight geometry and brittle nature of the carbon fibers makes them more prone to breakage during processing, which decreases the aspect ratio even more. Wen *et al.* suggest that hybrid systems with CB and CNT are processed in a manner that promotes the extension and orientation of CNT aggregates, which should result in a lower percolation threshold. [31]

The synergistic behaviour between particles is found to happen in different ways. It can be either a probabilistic advantage from the combination of different geometries, or the presence of a filler phase can contribute to the intrinsic properties of the other filler and vice versa. As an example of the latter, Zhang *et al.* have found that the aggregation of carbon nanotubes is partially inhibited with a very small addition of expanded graphite. In this study, also the geometrical advantage was present. [32] The following figure **figure** 4.4 represents different scenarios for a CB+CNT hybrid, where conductivity formation mechanisms $1-3$ are shown. First of the mechanisms is the connection of separate CNTs via CB agglomerate, the second is the co-formation of a junction point inside the active conducting network, and the third is the connection of CB agglomerates via CNT. The mechanisms are discussed in more detail by Sumfleth *et al* [29].

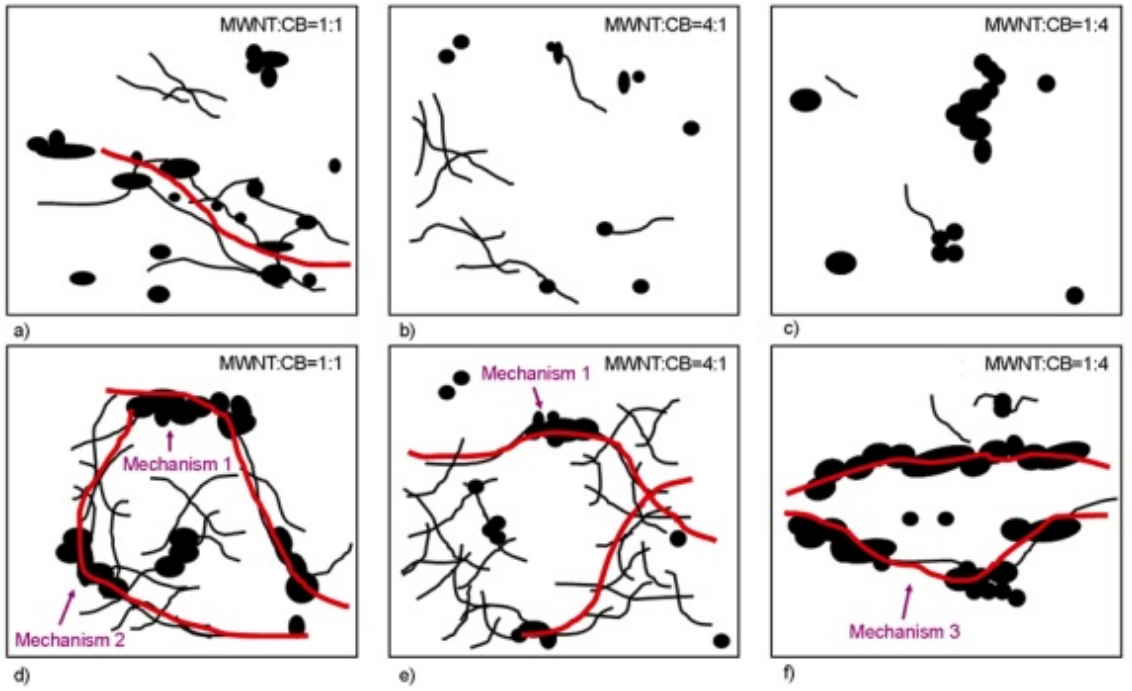

***Figure** 4.4 CNT+CB hybrid structures. In cases a-c the filler content is below percolation and in d-f it is exceeded. [33].*

Based on their results Zhang *et al.* consider that there is a correlation between the active mechanism and the filler weight fraction. Synergistic effects can be thought to be highest when all the mechanisms are active. Their results are consistent with the aforementioned theory, since a resistivity below $10^4\ \Omega cm$ was achieved with 0.5 wt-% using a CB:MWCNT weight ratio of 1, while over 2 wt-% was needed for the other specimen. Moreover, the measured conductivity at higher concentrations changed according to the ratio of fillers, which supports statement made in section 2.2, that filler's intrinsic conductivity defines the upper limit for the whole composite. [33]

The addition of an insulating filler to a hybrid filler system has been shown to enhance the electrical properties of the composite by decreasing the percolation threshold. One of the possible mechanisms proposed by Grunlan *et al.* is illustrated in **figure** 4.5 [34].

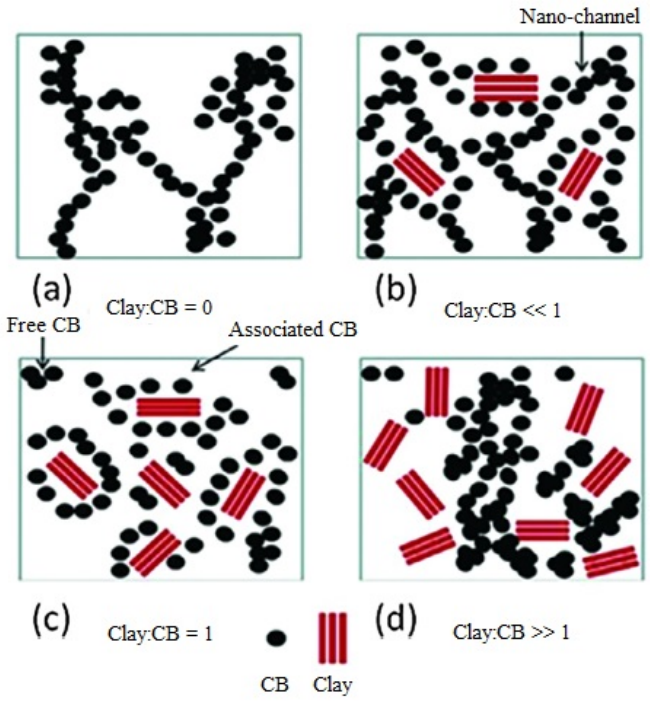

Figure 4.5 *Formation of different filler networks with different filler concentrations. Modified from [34].*

Control in dissipative region has been achieved by utilizing organic and inorganic fillers together with a constitution of 1 wt-% of CB (Ketjenblack EC 600 JD) and 10-25 wt-% of glass fibers [4, p. 209–217]. The level of conductivity was altered by incorporating carbon fibers to this hybrid filler system. The resistivity decreased considerably up to addition of 17 wt-% of CF.

5. RHEOLOGICAL ASPECTS IN FORMATION OF CONDUCTIVE NETWORKS

The melt processing methods for incorporating fillers into matrix and shaping of product are known to cause convergent flows, that affect to the conveying of fillers. Possible outcomes include orientation of particles and obstruction of particle networks [5, p.175–176]. On the other hand filler particles have different affinities towards polymers, which has led to planned utilization of polymeric blends in production of conductive materials.

During the melt processing CB is able to migrate from a phase to another, especially if it is initially compounded to the polymer with lower polarity. [17]

5.1 Phase inversion

A polymer blend consisting of a pair of immiscible polymers can exist in various morphologies, which include four basic types:

- Matrix-dispersed particle structures
- Matrix-fiber structures
- Lamellar structures
- Co-continuous structures

The depending outcome is dependent on kinetic factors including rheological properties, interfacial tension, blend composition and processing composition [35]. Co-continuous structures leads to better dimensional stability and even increases the maximum operational temperature of the material, when compared to dispersed morphology. The pronounced synergistic behaviour between the blend matrices has led to better mechanical properties and in the case of conductive fillers it provides a way for achieving a low percolation threshold.

Feng *et al.* have shown in their studies that by using a very high viscosity material, e.g. UHMWPE, as a blend component one can affect to the localization of carbon black particles [20]. **Figure** 5.1 is an optical micrograph of a 2 wt-% CB-filled blend with UHMWPE:PP ratio of 3/7. From the micrograph it can be seen that the type of morphology is matrix-dispersed. The white areas of UHMWPE are not being penetrated by carbon black particles, while small particles are thoroughly mixed inside the PP-phase. At the interface between UHMWPE and PP, a dark border can be seen, which implies that the local CB concentration is higher than within the PP phase.

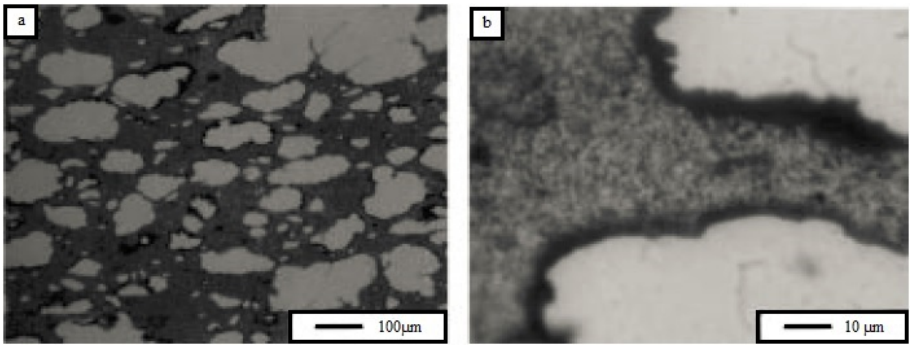

Figure 5.1 *An optical micrograph of a carbon black filled PP/UHMWPE blend with matrix-dispersed blend morphology. Modified from [20].*

In a sample with 10 wt-% of CB, the white *"islands"* remained, while the gray areas turned black, which is a clear indication of the CB's affinity towards the PP-phase after the interfacial area has been saturated [20]. The conductive paths in such blends are formed with two mechanisms: either the CB dispersed inside the PP-phase forms a network alone or it is formed together by the CB-rich interfaces and the PP-phase. Since the interfacial surface area increases proportional to the amount of UHMWPE, the mechanism which governs is influenced by the weight ratio of the polymers.

5.2 Compounding sequence

The final blend morphology and the locations of filler particles in the filled polymer blend depend partially on the order of compounding. The filler introduction can be done in multiple ways, it can be either sequential mixing or it can be done in a single stage process. The amount of blend components defines the possible methods - for a blend of 2 polymers the choices are to:

- Mix the filler into A/B, then add the other
- Mix the polymers, then add the filler
- Mix the filler into polymers A and B, then combine
- Mix everything simultaneously

The outcome will be such, that the filler is either in one phase, in both phases or at the interfacial region. If the filler is forced into polymer it does not have a good affinity with, it migrates out of the initial phase when adequate conditions are fulfilled.

5.3 Shear flow and its effect on fillers

In situations where a polymer melt is in between of moving and stationary elements, a shear profile is formed. The shear stress and rate are at highest on the stationary edges, while the flow rate is at its minimum - and for the moving edge it is the opposite. The melt flow can be thought to be laminar, for which reason polymer molecules and non-spherical fillers tend to align in the flow direction. Shear forces are known to break down agglomerated structures. Moreover, shearing is found to decrease the aspect ratio of fillers such as carbon fibers during processing [23, p. 327–328].

Shear flow has a different effect on fillers depending on their structure. Dispersive type of mixing is most effective on rigid particulate additives. For the behaviour of deformable particles the more governing factor is interfacial tension, which causes changes in miscibility to volume fraction and ratio of viscosity and elasticity between the additive and matrix. [36, p.636]

Ngabonziza *et al.* have studied the effect of injection velocity on the electrical and mechanical properties of MWCNT/PP nanocomposites [37]. Their samples were diluted with polypropylene into fixed MWCNT concentrations from a MWCNT/PP masterbatch containing 20 wt-% of nanotubes by using an injection molding machine. The studied injection velocities were 25.4 mm/s, 101.6 mm/s and 177.8 mm/s. While the injection speed was not found to affect the mechanical properties considerably, the electrical properties resulted in very different conductivities. Totally consistent behaviour was not observed, but a general trend is that at lower injection speeds the conductivities are nearly identical, but begin to separate when the injection speed is increased. The change between 25.4 mm/s and 101.6 mm/s is almost

negligible, but a further increase to 177.8 mm/s results in remarkable fluctuation. Concentrations 4.5 wt-%, 7 wt-% and 10 wt-% led to conductivities 5 times higher, some (4 wt-% and 12 wt-%) remained nearly unchanged and one (5 wt-%) was even noticed to decrease slightly. Their tests also included samples with concentrations 3.5 wt-% and below, but they remained insulating throughout the tests. The inconsistency is probably related to the poor mixing obtained with the dry blending, while it also indicates that the increased injection velocity facilitates the orientation process of the carbon nanotubes. From TEM micrographs it was seen that at the injection speed of 25.4 mm/s MWCNTs form agglomerated bundles, which at 177.8 mm/s are clearly elongated and even individual nanotubes can be observed.

In their studies of CF+CB hybrid filler in polypropylene matrix Drubetski *et al.* found that preferential fiber orientation in injection moulding was inhibited by the presence of carbon black particles. Also the fiber breakage was accelerated, when another filler was present during processing. Their tests included comparison tests with only fibers in two matrices of different viscosities. According to their results high viscosity promotes flow orientation and leads to higher percolation threshold values. However, the inhibiting effect of introducing carbon black to the system was strong enough to resist flow-induced orientation. [30]

Part II

Experimental part

6. MATERIALS

The compounding of the materials was carried out with a kneader-extrusion line, which is schematically illustrated in **figure** 6.1. The processing parameters were chosen to suit the rheology of both polymeric base blends, and the aim was to keep them invariant. Due to the different flow characteristics and other properties of the fillers, feeding became an issue since the amount of filler that could be fed into the mixture was limited. For some of the fillers either the throughput of the process had to be lowered or the compounding had to be done in multiple stages to obtain adequate filler concentrations. Changes in throughput lead to different dispersion qualities between compounds while the thermal history is different for the multi-stage processed compounds.

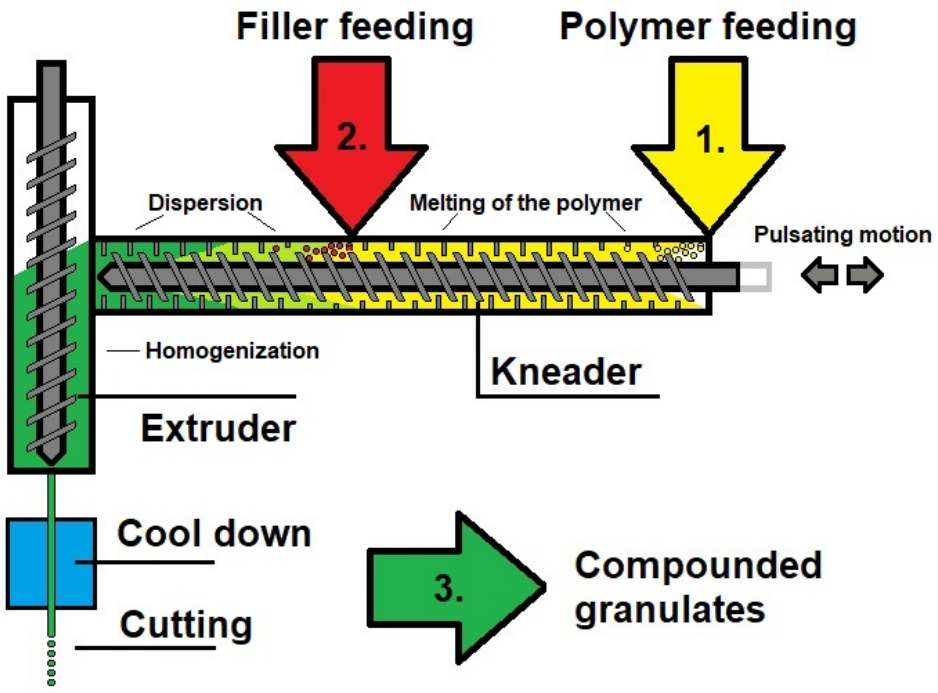

Figure 6.1 *Simplified presentation of the used kneader-extrusion line.*

The materials that are selected for further experiments are chosen based on their performance and other factors e.g. processing complexity, market demands and cost of the ingredients. Thus, the formulations that are selected to the second stage of the test plan are not chosen according to academic interest only.

6.1 Polymer blends

Two different polymeric bases were selected for this study: an olefin-based blend A and a polystyrene-based blend B. The ratios of blend constituents are listed in **table** 6.1. Separate tests were made with blend A, where the ratio of polymers was altered.

Table 6.1 *Polymer ratios of the blends*

Blend	Polymer 1	Polymer 2	Polymer 3
Blend A	80%	20%	-
Blend B	70%	20%	10%

6.2 Fillers

All of the fillers included in this study are commercial carbon-based fillers. Fillers A, B, D and E represent low aspect ratio fillers that differ in particle size and structure, while filler C has considerably higher aspect ratio. **Tables** 6.2 and 6.3 list the initial test compounds and targeted filler contents.

Table 6.2 *The target constitutions of the single filler compounds*

Sample ID	Blend	Filler A	Filler B	Filler C	Filler D	Filler E
TP16597	A	25%	-	-	-	-
TP16598	A	-	45%	-	-	-
TP16599	A	-	-	25%	-	-
TP16000	A	-	-	-	45%	-
TP16001	A	-	-	-	-	15%
TP16002	B	25%	-	-	-	-
TP16004	B	-	-	25%	-	-
TP16005	B	-	-	-	45%	-
TP16739	B	-	35.0%	-	-	-

The amount of possible hybrid filler combinations increases remarkably when the amount of different fillers is increased. Four fillers were tested in order to include multiple various filler combinations while keeping the workload in control.

Table 6.3 *The target constitutions of the initial hybrid filler compounds*

Sample ID	Blend	Filler A	Filler B	Filler C	Filler D
TP16681	A	15%	-	-	15%
TP16682	A	10%	-	10%	-
TP16683	A	-	-	14%	14%
TP16684	A	-	20%	-	20%
TP16685	A	-	10%	10%	-
TP16686	A	15%	15%	-	-
TP16687	B	14%	-	-	14%
TP16688	B	10%	-	10%	-
TP16689	B	-	-	15%	15%
TP16690	B	-	21%	-	21%
TP16691	B	-	10%	10%	-
TP16692	B	15%	15%	-	-

As it can be seen from the table above, there are few combinations (TP16683, TP16687 and TP16690) with slightly differing contents from the rest. These changes were made based on the flowing characteristics of the fillers and the surface resistance values of the specimen that were measured on-the-go.

7. METHODS

In this chapter the analysis methods and the details about sample preparation are introduced. The main interest is on the surface resistance measurements, while other methods are used to assess the effect of various factors on the formation of surface conductivity. Since the amount of filler combinations to be tested in this study is high, some important choices were made prior to beginning:

- The blend constituents' weight ratios were kept constant despite the different filler contents.
- The preliminary tests are done with filler:filler ratio of 1.
- The compounding process is fixed with slight necessary alterations depending on the flow characteristics of the fillers.
- The percolation graphs were measured by dilution from a concentrate.

The reasons for using the weight ratio of 1 are a) it is simple and b) it is the same for all, which makes the comparison less complicated. Another option would have been to use the relative conductivity of the fillers, which would require precise information about the percolation thresholds. Most of the hybrid fillers were compounded as a single stage process with some exceptions due to large differences in filler densities. All of the percolation curves were formed with a dilution process; Compounds with excessive filler content were manufactured and subsequently diluted to lower concentrations in either an injection moulding machine or an extruder. The necessary alterations include slight changes in the throughput rate since each filler has its own feeding factor in the gravimetric feeding unit, and thus some materials cannot be produced in a fully comparable manner.

Physical blending of polymers is a fast and cost-efficient way to tailor the properties of polymer-based materials. In blend formulation a polymer with roughly the desired properties is chosen, which is then modified by adding ingredients that tweak the material to some direction. The properties change according to the relative

quantity of an ingredient and it's attributes. The ingredients are likely to interact with each other, thus the performance will not necessarily be a simple resultant of the ingredients' properties. The process of melt mixing polymers and additives, to form a continuous multicomponent structure with desired properties, is called compounding. In order to get a good quality compound following processing parameters should be considered [3]:

- *Throughput* i.e. capacity affects to the amount of shear stress that is transferred to the polymer melt.
- *The screw speed* defines the shear rate, which can have an effect on the throughput due to shear thinning flow behaviour.
- *Screw configuration* is an important factor, which defines the degree of dispersive and distributive mixing.
- *Processing temperature* affects directly to the melt's ability to flow.

The type of multiphase structure and morphology is a result of processing conditions and affects to the properties of the compound [36]. The effects of changing these parameters should be studied, if the material is to be thoroughly characterized. The dissipative transition describes the area, where charge transportation is easy, but either the carrier concentration is low, their mobility is hindered or the potential difference is too small to tunnel through the extrinsically conductive material. Steep dissipative curve implies, that the charge transfer is efficient if the particles are able to form a network. Gentle slope, on the other hand, results when a slight addition to percolating material only increases its efficiency slightly by 1) shortening the path from electrode to another or by 2) increasing the amount of charge carriers.

The compounding is done with a reciprocating single screw extruder (kneader). In the processing line the polymer is melted within a kneader unit, where the a back and forth pulsating screw conveys and plasticizes polymer granulates. Into this melted polymer a filler is introduced via a gravimetric side feeder. Both constituents are eventually transported to a crosshead unit, which is a small single screw extruder with a circular extrusion die at its end.

7.1 Ash content measurements

Ash content measurements of filled plastics are based on different decomposition temperatures of chemical substances. In elevated temperature material is removed

from the sample crucible due to its decomposition or chemical interaction with the adjacent molecules. By using nitrogen as the testing atmosphere, carbon-based fillers remain intact while the polymer matrix is decomposed. The ash of a filled polymer consists of the remaining filler content and char. Charring occurs for some polymers, which means that the polymer is not entirely removed under nitrogen atmosphere. The amount of charring depends on the chemical structure, for some polymer grades it can be significant, and thus char should be removed under Oxygen atmosphere. [38]

The filler content of the samples was confirmed with a set of 3 residual content measurements in 600 °C within nitrogen atmosphere per compound. The sample size was 10–20 granulates, and approximately 0.5 grams by weight. The samples were cooled under air for 10 ± 3 minutes, and subsequently weighted. The role of these measurements is to backup, whether the gravimetric feeding unit of the extrusion line is to be trusted.

7.2 Surface resistance measurements

Surface resistivity is a material property that describes the amount of electrical resistance the material causes per surface area under electrification. In surface resistance measurements the surface layer is assumed to convey all the charge despite some of the charge being transmitted within the material. The measured resistance value is affected by measurement voltage, electrification time and ambient humidity. Also the measurement platform's conductivity transforms the measured values. By using higher voltage or carrying out the measurements in higher humidity, lower resistance values are obtained. Increased electrification time leads to charging of the material, which increases its resistivity. The set up for a surface resistance measurement with a bar electrode is schematically represented in **figure** 7.1.

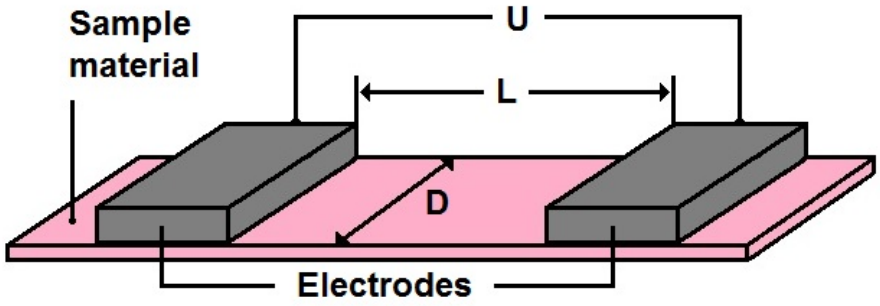

Figure 7.1 *Illustration of a SR measurement for film with a bar electrode*

The surface resistivity of a material, can be expressed as

$$\rho_s = \frac{U/L}{I_s/D} \tag{7.1}$$

where U is the measurement voltage, I_s is the surface current, D is the width of the electrode and L is the span between the electrodes. If the L/D ratio of the probe is 1, then the measured surface resistance is equal to material's surface resistivity. If the dimensions between the electrodes are not considered, the measured quantity is the surface resistance of an object. The testing process has been standardized with ASTM D-257 and ANSI ESD S11.11:1993 standards. The former is for DC resistance measurements for insulating materials, while the latter is for surface resistance measurements of dissipative planar materials.

The specimen are either injection moulded tensile test specimen or extruded tapes. Dry blends of 600 grams were weighted for each dilution. The injection moulded (blend A) specimen were collected from four subsequent injection cycles after the process has stabilized. The surface resistance measurements were made from 2 pairs of samples from their both flat sides. The extruded (blend B) compounds were measured from the both sides of the extruded tape. A surface resistance metering device (SRM200) was used. The measurement voltage was 10 V for resistivities below 10^6 Ω and 100 V for higher resistivities. Since the compounds are unlikely to be perfectly homogeneous after being processed to their final shapes, the surface resistance of the object is a more describing property to study than material resistivity. The follow-up studies include thermoforming of selected specimen, for which different probes were used in the surface resistance measurements. A small circular-headed single point probe and a pair of small rubber electrodes shown in **figure** 7.2 were used together with a different surface resistance meter due to probe incompatibility with the SRM200. The rightmost electrode is the bar electrode, that was used for the majority of the SR testing.

Figure 7.2 *Different SR measurement probes, that were used in this thesis*

Prior to thermoforming, plastic sheets had to be extruded, thus approximately 8 kg of material was compounded and subsequently extruded. The sample sheets were collected after the line stabilized and produced extrusion film with a consistent quality. In **figure** 7.3 a thermoformed specimen is shown.

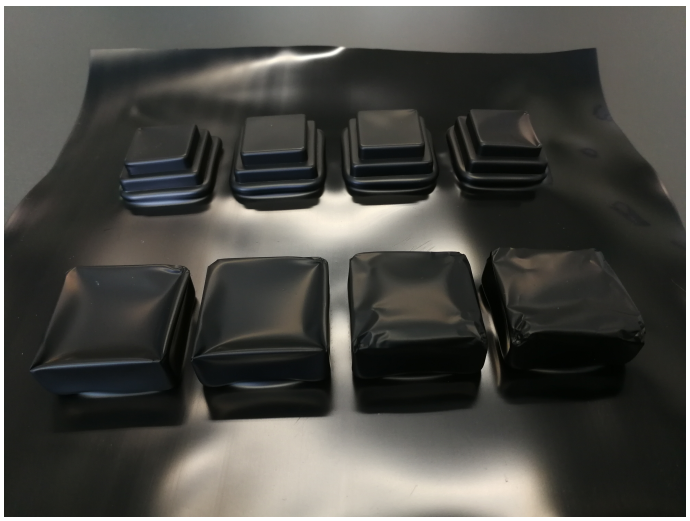

Figure 7.3 *Thermoformed extrusion sheet*

7.3 Scanning electron microscopy, SEM

In optical microscopy the images are formed by reflected light, whereas in electron microscopy electrons are used. In comparison, electron microscopes offer better

resolution and higher magnifications, which are necessary for making observations on the filler dispersions. **Figure** 7.4 shows a schematic illustration of a scanning electron microscope.

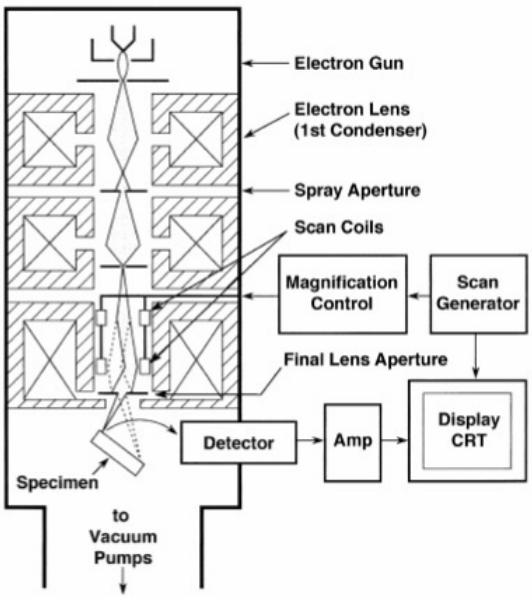

Figure 7.4 *Schematic presentation of SEM's electron column [39, p. 23].*

The electron gun produces electrons, that are accelerated with a certain acceleration voltage, that defines the kinetic energy of the individual electrons. The formed beam of electrons is guided and focused with magnetic lenses and apertures. The electrons, which hit the sample surface produce different kind of signals such as secondary (SE) and backscattered electrons (BSE), which can be detected and used to form the microscopic image. The data is collected from an interaction depth, that exceeds well below the surface, thus it should be known that the contrast formation is not limited to only topographic details.

The model of the used SEM apparatus is Zeiss ULTRA plus. The SEM samples were prepared for imaging according to following guidelines. First the desired parts of the specimen are cut into smaller pieces that can be cold-mounted by using a two component epoxy resin. These mounted specimen are ground with abrasive papers made of silicon carbide and polished with $3\mu m$ polycrystalline and $1\mu m$ monocrystalline diamond suspensions. The sample surfaces are cleaned from abrasive residue with ethanol. The sufficient quality of polishing is verified with an optical microscope prior to SEM.

The SEM-studies in this thesis are included to make observations on the dispersion quality, and to assess different particle structures and morphological details on

the studied specimen. With surface resistance measurements the absolute performance of the specimen can be compared, while electron microscopy might provide explanations for why different behaviour patterns exist.

7.4 Differential scanning calorimetry, DSC

Differential scanning calorimetry is an analysis method, where a small ($\approx$ 10 mg) representative sample is subjected to a thermal program together with a reference sample while measuring the heat input required to cause a change in temperature. With DSC it is possible to observe chemical reactions and physical changes that are exothermic, endothermic or affect to the heat capacity of the material. Typical polymeric phenomena that are studied with DSC include crystallization, melting and glass transition. The crystallinity of a pure polymer is

$$\%Crystallinity = \frac{\Delta H_{melting} - \Delta H_{cold\ crystallization}}{\Delta H_{100\%}} \tag{7.2}$$

In the case of polymer blends the reference value for 100% crystallinity cannot be accurately defined, since different polymers have their own enthalpies for crystallizations. The rule of mixture does not apply since multiple abundant phases hinder the ability of a sole polymer to form crystalline regions. However, rough estimations on the degree of crystallinity can be made based on the enthalpy values of the melting peaks. Within this thesis DSC is used for confirming the net effect of altering the ratio of blend constituents, which is done in a manner that affects to the degree of crystallinity. **Table** 7.1 lists indirect estimations of the 100% crystallinity enthalpies for common linear thermoplastics.

Table 7.1 *The crystallinity reference values for common thermoplastic polymers. [40]*

Polymer name	**Acronym**	$\Delta H_{100\%}$ [J/g]
Polyethylene	PE	293
Polypropylene	PP	207
Polybutylene	PB	125
Polymethylenoxide	POM	326
Polyethyleneoxide	PEOX	197
Polycaprolactam	PA6	230
Poly(hexamethylene apidamide)	PA66	226
Poly(ethylene terephtalate)	PET	140
Poly(vinylidene fluodire)	PVDF	105
Poly(etheretherketone)	PEEK	130

8. RESULTS AND DISCUSSION

In this chapter the results obtained with the preceding methods are revised. The results are presented in a chronological order beginning with the initial single and hybrid filler studies, after which the chapter proceeds to the follow-up studies.

The approach that was used in this R&D study set its limitations on the analysis since more thorough testing should be done for more detailed information. The uncertainties are mainly caused by the assumptions that were mentioned in the earlier introduction. The method of forming the percolation curves from the concentrates brings uncertainty to the comparison since it is difficult to get data points, that are well comparable due to the sudden behaviour changes in the material within the dissipative region. Resistivity levels 10^6 Ω and 10^9 Ω were chosen as the lower and upper limits - and since the values obtained with the measurements range over the $10^3 - 10^{12}$ range, the filler contents that match the set resistivity levels have to be extrapolated from the nearest values. For some compounds either the dissipative area is too narrow or the dilution process causes too much deviation in the filler contents, in order to achieve the targeted resistance levels.

8.1 Single filler systems

Prior to beginning of the experimental part, the electrical behaviours of the fillers in these matrices and processing conditions were unknown, thus the experimentation had to begin with the characterization of the single filler systems. The measured filler contents for these compounds are listed in **table** 8.1 and the surface resistance measurement data are plotted in figures 8.1 and 8.2.

Table 8.1 *The measured average constitutions of the initial single filler compounds*

Sample ID	Blend	Filler A	Filler B	Filler C	Filler D	Filler E
TP16597	A	24.8%	-	-	-	-
TP16598	A	-	44.9%	-	-	-
TP16599	A	-	-	24.6%	-	-
TP16000	A	-	-	-	44.0%	-
TP16001	A	-	-	-	-	15.2%
TP16002	B	26.2%	-	-	-	-
TP16004	B	-	-	24.8%	-	-
TP16005	B	-	-	-	44.0%	-
TP16739	B	-	36.1%	-	-	-

When the above filler content values are compared to the targeted values listed in **table** 6.2, it can be seen that the values are reasonably close to each other with only a 1.1 wt-% error at highest, thus the feeding unit of the extrusion line can be trusted. Even if the filler content would be slightly off, its effect will be nearly negligible since the dilution process treats the data points in a similar way, and when combined to the fact that the interest is mainly in the width of the dissipative region and not in the exact filler content values. The percolation curves are plotted below in figures 8.1 and 8.2 for blends A and B, respectively.

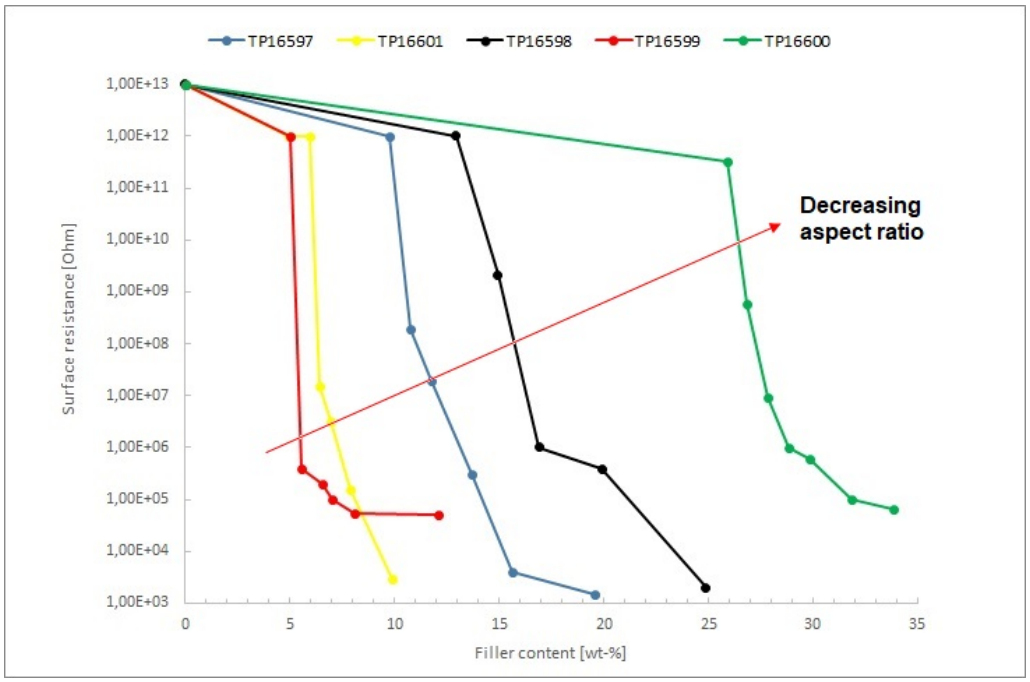

Figure 8.1 *The percolation curves of Blend A single filler compounds*

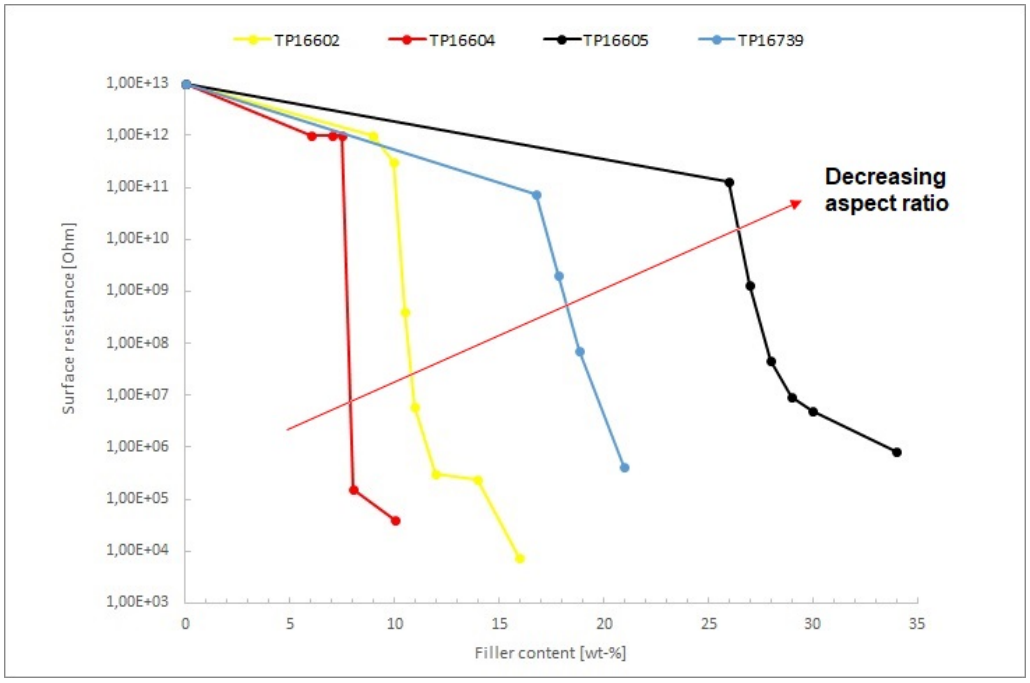

Figure 8.2 *The percolation curves of Blend B single filler compounds*

Except for the filler E that was tested only in blend A, the above figures include the same fillers in two matrices, and they are quite well distinguishable as the curves have a similar shape near the same values. Also the trend can be seen, that the curves in **figure** 8.1 are located at lower filler contents except for TP16597 and TP16602. This difference is probably due to filler structure breakdown under injection moulding, i.e. the shear forces are low enough to retain the filler network in extrusion.

The dissipative regions of the studied specimen are described in **table** 8.2 with values that have been calculated with linear extrapolation based on the results in appendix A. The process of obtaining comparable data points became an issue, thus the comparison is done based on both the change in SR and change in filler content to provide more descriptive analysis. **Figure** 8.3 shows the different scenarios that were confronted upon extrapolation of the data. The ΔSR value equals to the difference in the surface resistances of the two data points that are used to form the slope. If ΔSR is 3.0, it means that the coefficient is formed between datapoints of 10^6 Ω and 10^9 Ω as it was meant to be done. If the value is 6.0, then the upper datapoint is lacking and the coefficient is formed between the extrapolated 10^6 Ω value and a filler content, at which the resistivity is higher than the upper limit 10^{12} Ω of the measurement device. For materials, with the value higher than 6.0, the comparison is made between the two known measurement points instead of extrapolation due to linear extrapolation resulting in clearly false values.

Table 8.2 *The coefficient and width values that describe the dissipative areas of the single filler systems*

Sample ID	**Blend** ΔSR	Δ Filler content [log(Ω)]	Coefficient [wt-%]	
TP16597	A	6.0	3.4	-1.8
TP16598	A	3.0	1.8	-1.7
TP16599	A	6.0	0.9	-6.5
TP16600	A	3.0	2.1	-1.4
TP16001	A	6.0	1.4	-4.4
TP16002	B	3.0	1.2	-2.5
TP16004	B	6.8	0.5	-13.6
TP16005	B	3.0	6.4	-0.5
TP16739	B	3.0	2.6	-1.2

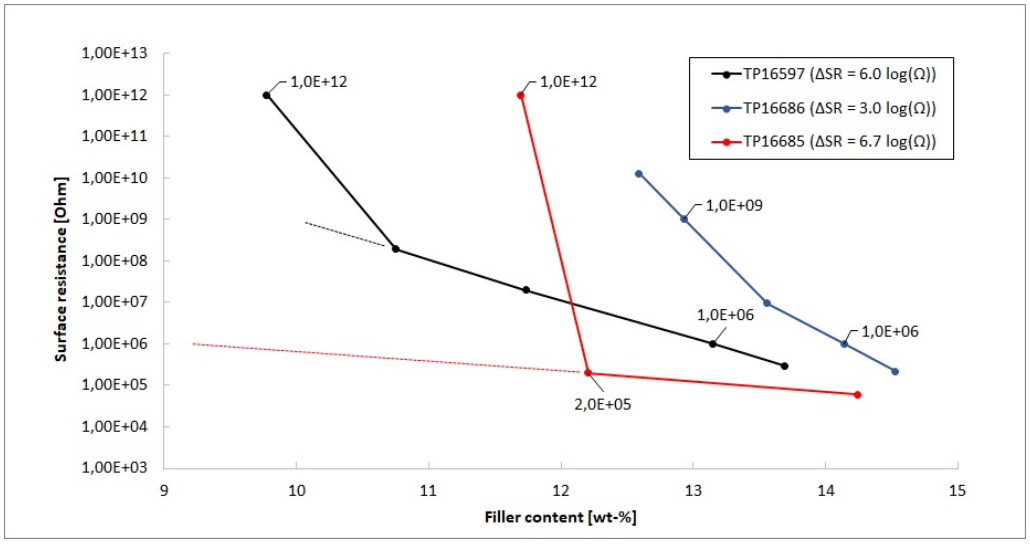

Figure 8.3 *Examples of the three different cases, where ΔSR values are different.*

The compounds incorporating filler C (TP16599, TP16004) with its high aspect ratio stands out by having the steepest percolation transitions, while fillers B and D seem to exhibit gentle transitions with notable steepness increments in the blend B when compared to the blend A formulations. The data point iteration for fillers A and E was partially unsuccessful due to final resistance being significantly lower after cool down and conditioning of the specimen. The filler E (TP16001) is likely to have the second steepest transition of the studied fillers as the change from 10^6 to over 10^12 occurs within the margin of less than 1.4 wt-%. Filler A shows quite promising behaviour despite the unsuccessful upper data point. Further more, it is the only filler that might exhibit better results in the blend A. For the filler A a breakdown of the filler structure is to be expected, which might work out in a positive manner in this case. Overall, it would seem that the fillers with either high

aspect ratio or low percolation threshold yield the steepest percolation curves, and the effect is enhanced if the processing method is such that structural breakage does not occur.

8.2 Hybrid filler systems

The individual fillers A-D were combined to form 12 hybrid filler systems, whose results are reviewed in this chapter. The compositional details of the produced compounds are listed in **table** 8.3. In figures 8.4 and 8.5, the percolation curves are presented.

Table 8.3 *The measured average filler contents of the initial hybrid filler compounds*

Sample ID	Blend	Filler A	Filler B	Filler C	Filler D
TP16681	A	12.5%	-	-	12.5%
TP16682	A	10.3%	-	10.3%	-
TP16683	A	-	-	13.4%	13.4%
TP16684	A	-	20.5%	-	20.5%
TP16685	A	-	10.0%	10.0%	-
TP16686	A	14.8%	14.8%	-	-
TP16687	B	14.3%	-	-	14.3%
TP16688	B	11.3%	-	11.3%	-
TP16689	B	-	-	14.1%	14.1%
TP16690	B	-	21.7%	-	21.7%
TP16691	B	-	10.9%	10.9%	-
TP16692	B	15.8%	15.8%	-	-

The largest difference to the values in **table** 6.3 was 1.3 wt-%, if TP16681 is excluded. The deviations are close to the ones observed in single filler compounds. The lower filler content of TP16681 can be explained with insufficient filler feeding due to combination of poor feeding characteristics and unnecessarily high target value. Despite having lower than intended initial filler content, the percolation curves could be formed from each of the specimen.

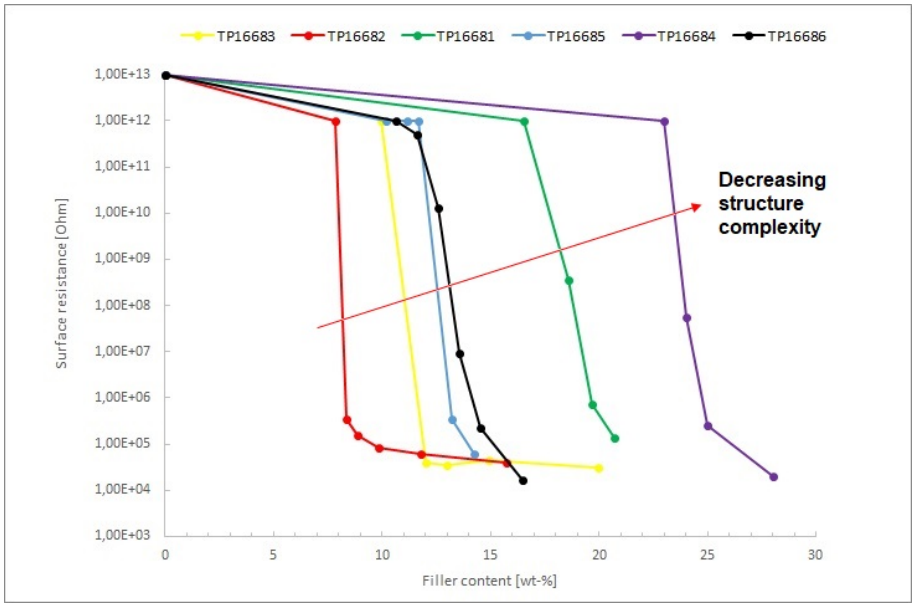

Figure 8.4 *The percolation curves of Blend A hybrid filler compounds*

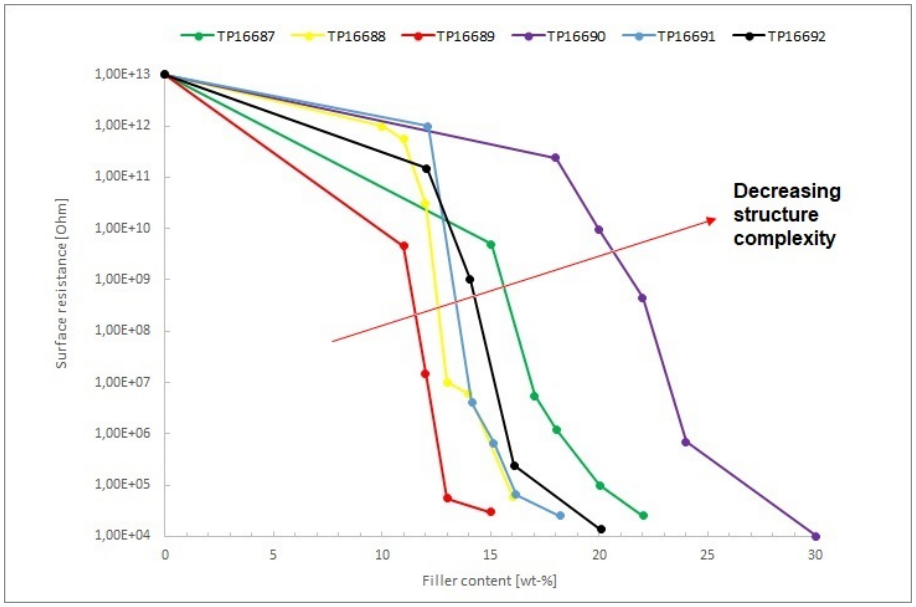

Figure 8.5 *The percolation curves of Blend B hybrid filler compounds*

As it can be seen, the sudden changes in **figure** 8.4 are more controlled in **figure** 8.5, which again might be related to either the difference in processing method or polymer blend composition. TP16686 unlike its the single filler compounds (TP16597, TP16598) in blend A, resulted unexpectedly in much steeper dissipative region. The incorporation of filler B would intuitively enhance the breakdown of filler A's structure during the initial dispersing. Either the reason for differences between TP16597 and TP16602 are not caused by structural breakdown or there exists a mechanism

that promotes the formation of conductive paths. As it was expected, the hybrid compounds with filler D are the least conductive, except when combined with highly conductive filler C. The more conductive hybrid specimen are more interesting in this case, as the fillers A and C were the most conductive fillers alone, but the combination of these was the most conductive hybrid filler compound only in the blend A. The Blend B's most conductive hybrid filler compound was TP16689 despite incorporating filler D, which was individually the least conductive filler. The order of the curves is shown in **figure** 8.6 for both of the blends according to the conductivities of the different hybrid filler combinations. The resulting order is nearly logical as the conductive behaviour decreases according to the ingredients' properties. The three most conductive compounds include filler C, which was the most conductive individually, however, the order is not according to the second fillers' conductivities. Filler B is more conductive than filler D, but in the hybrid combinations with filler C, its introduction barely improves the conductive behaviour while filler D seems to have a remarkable increasing impact on conductive path formation. Explanations for that could be differences in filler orientation, filler dispersion, blend morphology or uneven feeding of the fillers. If the reason for the difference in percolation thresholds of TP16599 and TP16604 is related to breakage or orientation of fillers during injection moulding, then a probable cause for the different order could be the synergistic behaviour of the fillers. **Table** 8.4 is the hybrid filler compounds' equivalent of **table** 8.2 with the values describing the steepness of the dissipative region $10^6 - 10^9\Omega$.

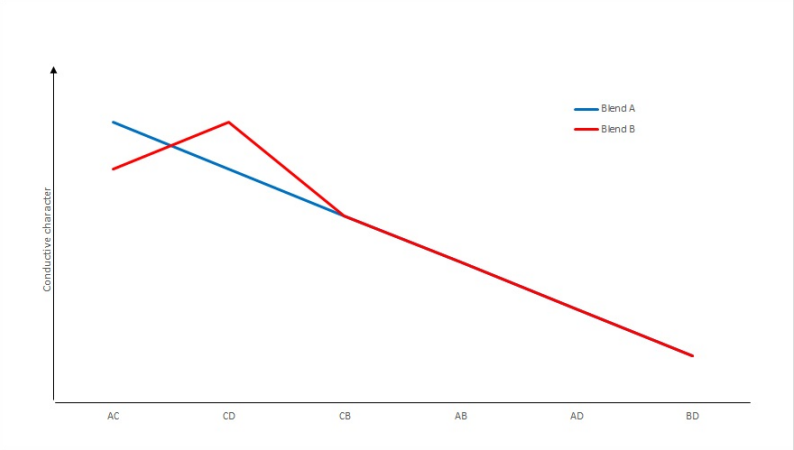

Figure 8.6 *The order of conductivity for different filler combinations in both of the blends blend.*

Table 8.4 *The coefficient and width values that describe the dissipative areas of the hybrid filler systems*

Sample ID	**Blend**	Δ Surface resistivity [log(Ω)]	Δ Filler content [wt-%]	Coefficient
TP16681	A	3.0	1.0	-2.9
TP16682	A	6.8	0.5	-13.9
TP16683	A	7.4	2.0	-3.7
TP16684	A	6.0	1.7	-3.4
TP16685	A	6.7	0.5	-13.2
TP16686	A	3.0	2.7	-1.1
TP16687	B	3.0	2.6	-1.2
TP16688	B	3.0	1.6	-1.9
TP16689	B	3.0	1.2	-2.5
TP16690	B	3.0	2.0	-1.5
TP16691	B	6.0	2.8	-2.1
TP16692	B	3.0	1.7	-1.8

As shown in **table** 8.4 the problems arise with the blend A formulations. The blend B specimen in comparison yield wide filler content ranges with TP16689 having the lowest value of 1.2 wt-%, which can be considered as a good improvement if the gap of less than 0.5 wt-% for TP16604 is taken into account. The effect of introducing the second filler with filler C does not seem logical, as the steepness of the transition is higher with filler D than with fillers A or B, which both are more conductive.

The reason for many combinations of filler A or C and B or D resulting in steeper than assumed behaviour could result from the increased amount of free electrons in the system. This would seem to apply for the specimen with fillers B and D as they are the least conductive hybrid filler configurations with transition widths that are among the highest of the studied materials.

8.3 Follow-up studies

The earlier chapters compared the different combinations while in this chapter few selected tests are reviewed. The division to initial and separate tests was made in order to emphasize the different aspects that were assessed since the results of this section provide additional information to support the analysis of the initial tests, but do not comprehensively explain the reasons behind the compounds' performance.

8.3.1 The effect of thermoforming

From the combinations of **table** 8.4, TP16692 was chosen for the testing due to most of the other hybrid combinations being industrially not suitable for the intended applications. Further testing was conducted prior to the thermoforming with filler weight ratios of 1:2 and 2:1. Targeted and measured filler contents of the compounds are listed in **table** 8.5, and in **figure** 8.7 the percolation curves are presented.

Table 8.5 *The formulations and measured ash contents of TP16692 with modified filler ratios*

Sample ID	Blend	Filler A	Filler B	Total ash content
TP16753	B	13.3%	6.7%	21.4%
TP16754	B	8.3%	16.7%	22.0%

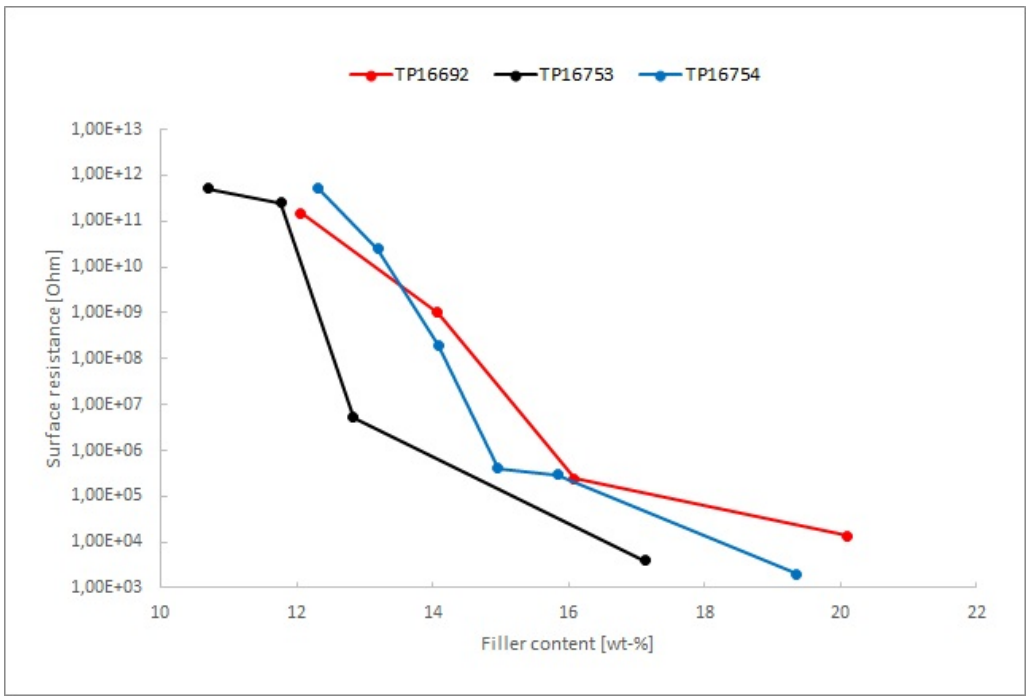

Figure 8.7 *The percolation curves for TP16753, TP16754 and TP16692*

For these compounds the feeding did not meet the target values as well as with the previous compounds. The reason for this change remains unknown as the parameters nor the actual readings were not significantly different from the ones used or observed during the processing of TP16692. **Figure** 8.7 shows that the behaviour changes with the filler ratio. The more conductive filler A is dominant when its ratio is 2 to 1, while no implications of filler B leading to more transient percolation curve can be seen. This would suggest that the filler ratio of 1 was a good assumption for fillers A

and B. It could be due to their relatively small difference in percolation thresholds, in which case the filler ratio should be altered for the other filler combinations.

The conductive behaviour after thermoforming was studied for all of the three above-mentioned formulations with an assumption that thermoforming is likely to decrease the conductivity of a material due to breakage of conductive paths. The results of the thermoforming tests are shown in **figure** 8.8, which shows slight differences in the thermoforming behaviour. The differences are too subtle for reliable comparison since the average resistivities of the thermoformed specimen are well within the standard deviation ranges of the reference specimen. The higher amount of filler A seems to increase the materials' susceptibility to breakage of conductive paths, which is probably due to filler A's structural character being broken under extension. The specimen were initially very conductive, thus the amount of stretching was insufficient to cause more visible damage to the conductive network. The overall result would be, that all of the studied specimen remained well conductive and could certainly be used in similar thermoformed applications, where efficient charge transportation is required.

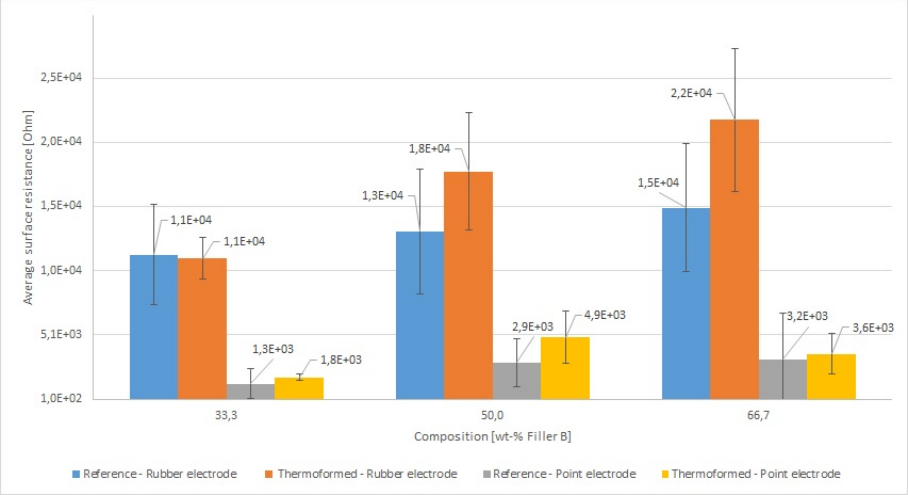

Figure 8.8 *Thermoforming results measured with the rubber and point electrodes as a function of filler ratio*

8.3.2 SEM results

The SEM studies could not offer observations to explain the performance of different hybrid filler combinations. One of the interests was to get information of the morphological differences between blends A and blend B, but the blend constituents were similar enough to form apparently homogeneous matrices. The background shows

irregularities, but no clear deductions can be made about fillers' preferential locations due to the lack of phase separation as shown in **figures** 8.9 and 8.10. Both abundant fillers are clearly visible in the above figure with no signs of agglomeration. The good dispersion quality indicates that an adequate degree of mixing was achieved.

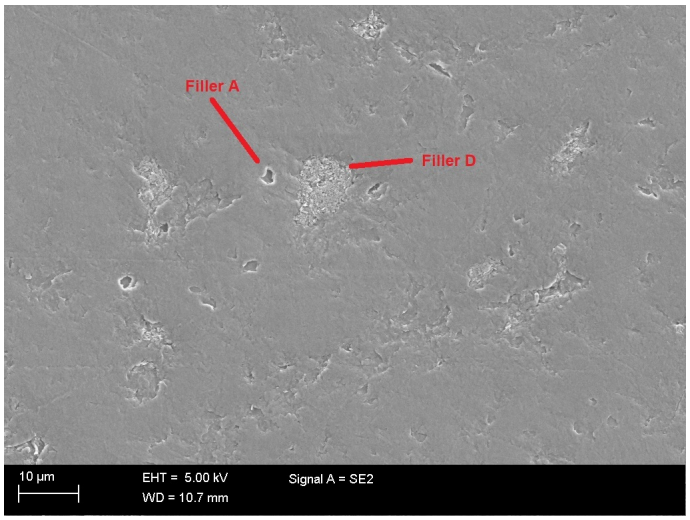

Figure 8.9 *SEM-micrograph of TP16681*

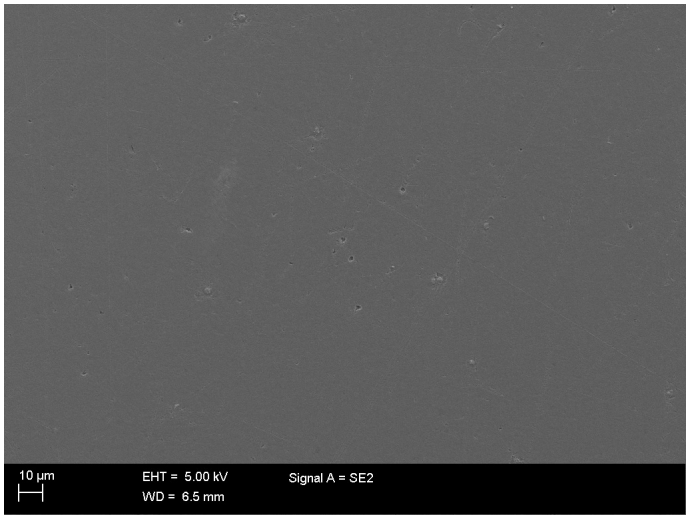

Figure 8.10 *SEM-micrograph of TP16753*

Similar to the earlier figure, the filler particles are well separated. The less distorted background implies that the polishing of the sample was successful, which is probably due to differences in hardness. In **figure** 8.9 it can be seen that filler A is much smaller in size in comparison to filler D. As both particles are similar in aspect ratio and their intrinsic conductivities are not far apart, the main factor defining the performance is the specific surface area, i.e. the particle size.

8.3.3 DSC results

Table 8.6 shows the compounds that were produced in order to assess the effect of modifying the polymer 2 content of TP16598, which is ought to affect the degree of crystallinity of the polymer blend. The degrees of crystallinity were calculated from the samples containing approximately 17 wt-% filler B by using the **eq.** 7.2 with the measured enthalpy values and reference values listed in **table** 7.1. The percolation curves and the measured crystallinities are presented in **figure** 8.11.

Table 8.6 *The formulations and measured ash contents of TP16598 with modified polymer 2 content*

Sample ID	Polymer 2	Filler B	Ash content
TP16751	10.0%	30.0%	30.2%
TP16752	20.0%	30.0%	30.0%

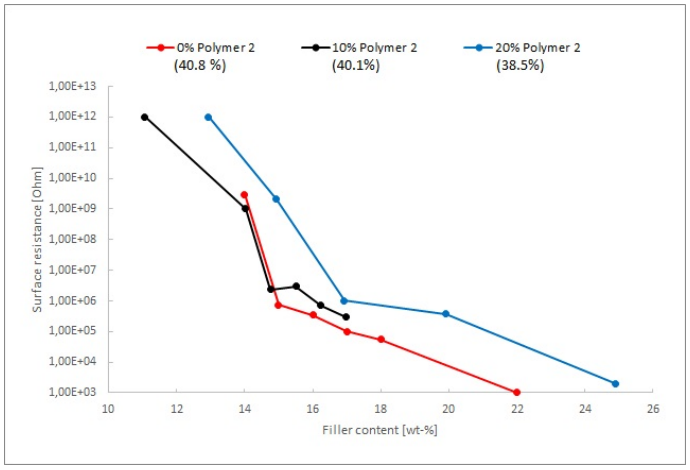

Figure 8.11 *The percolation curves for TP16751, TP16752 and TP16598*

It was assumed, that crystallinity changes the materials behaviour by forming crystalline segments that are impermeable to filler particles, which concentrates the fillers into the amorphous regions of the semi-crystalline material. The achieved changes in the degree of crystallinity are very subtle, thus the percolation curves are rather similar, but a trend that agrees with the assumption can be seen. With higher ratio of polymer 2, the crystal growth is hindered, which results in a more controlled transition and higher resistivity values within the studied range. The difference between 0% and 10% additions is practically negligible, but when compared to the 20% addition of polymer 2, the difference becomes evident.

9. CONCLUSIONS AND FUTURE ASPECTS

The main aim of the thesis was to study whether or not certain hybrid filler combinations provide possible benefits in controlling of the electrical properties. More insight was gained on how to proceed with the future experiments despite not finding a perfect solution for the industrial application. More thorough information was gained on how to proceed with the studies. The most relevant observations for the studied systems were:

- Low percolation threshold translates to steep dissipative region - and vice versa.
- The resistivity obtained with a hybrid filler correlates with the fractions and resistivities of the individual fillers.
- A decrease in the degree of crystallinity results in higher percolation threshold and resistivity.
- Extruded compounds yielded more transient percolation curves over injection moulded.
- The components of the polymeric blends were compatible, thus microscopical studies did not show signs of phase segregation.

Injection moulded compounds exhibited steeper percolation curves, which is either due to higher degree of crystallinity or the processing method. Polymeric blends with similar filler concentrations, but different crystallinities, were observed to have differences in conductivity. High crystallinity seems to promote the formation of conductive paths. The materials, which incorporated fillers of lower aspect ratio, offered the most transient behaviour when single filled. In the hybrid formulations there was some fluctuation in the order of transition steepness, but the overall trend was similar to the single filler systems: Low aspect ratio and filler structure combinations yielded more gentle transitions and higher percolation thresholds. Interestingly, Filler B yielded a consistent and wide transition, while the specimen with filler D had wide insulative to conductive -transition that subsides at rather high increments of

filler. The combinations of two fillers with higher and lower conductivities had rather steep percolation behaviours with the filler/filler ratio of one.

These test formulations provided quick answers whether or not certain combinations are industrially interesting or applicable, but in academic mind the background testing was insufficient to draw more general conclusions. Next stage of the testing would depend on the aim. If its knowledge of the mechanisms that is pursued, then a) different ratios of blend constituents should be tested, b) both of the blends should be processed with similar methods, c) the effect of crystallinity should be studied with higher amounts of polymer 2 and d) thermoforming tests should be continued with either more filler combinations or with higher initial resistivity samples. Furthermore, the true potential of the studied fillers remains unsolved, since the filler ratios were altered only for the samples containing fillers A and B. Especially in the case of filler C, the achieved conductivities were excellent and the specimen had steep dissipative regions, for which reason they were deemed as not of interest despite the possibility of achieving better performance with more suitable filler ratios. The determination of percolation thresholds and compounding of specimen with filler ratios matching their relative conductivities is time consuming, but it would provide percolation graphs, that treat all of the fillers in the same manner.

REFERENCES

[1] M. Mansfield and C. O'Sullivan. *Understanding physics*. Wiley, 1999.

[2] E. Riande and R. Diaz-Calleja. *Electrical properties of polymers*. Marcel Dekker, Inc., 2004.

[3] iPolycond Consortium. *Introduction to conductive polymer composites*. Smithers Rapra Technology, 2011.

[4] L. Rupprecht. *Conductive polymers and plastics*. Plastics design library, William Andrew Inc., 1999.

[5] J. L. Leblanc. *Filled polymers: Science and industrial applications*. CRC Press, 2010.

[6] L. B. Tunnicliffe, J. Kadlcak, M. D. Morris, Y. Shi, A. G. Thomas, and J. J. C. Busfield. Flocculation and viscoelastic behaviour in carbon black-filled natural rubber. *Macromolecular materials and engineering*, 299:1474–1148, 2014.

[7] N.C. Das, D. Khastgir, T. K. Chaki, and A. Chakraborty. Electromagnetic interference shielding effectiveness of carbon black and carbon fibre filled eva and nr based composites. *Composites: Part A*, 31:1069–1081, March 2000.

[8] Y. Chen, F. Pan, S. Wang, B. Liu, and J. Zhang. Theoretical estimation on the percolation threshold for polymer matrix composites with hybrid fillers. *Composite structures*, 124:292–299, January 2015.

[9] I. Balberg, C. H. Anderson, S. Alexander, and N. Wagner. Excluded volume and its relation to the onset of percolation. *Physical review B*, 30(7), October 1984.

[10] Y. Sun, H-D. Bao, Z-X. Guo, and J. Yu. Modeling of the electrical percolation of mixed carbon fillers in polymer-based composites. *Macromolecules*, 42:459–463, November 2009.

[11] U. Szeluga, B. Kumanek, and B. Trzebicka. Synergy in hybrid polymer/nanocarbon composites. a review. *Composites: Part A*, 73:204–231, February 2015.

[12] S. Asai, K. Sakata, M. Sumita, and K. Miyazaka. Effect of interfacial free energy on the heterogeneous distribution of oxidized carbon black in polymer blends. *Polymer journal*, 24(5):415–420, 1992.

[13] G. T. Barnes and I. R. Gentle. *Interfacial science: an introduction.* Oxford University Press Inc., 2011.

[14] C. Zhang, X. S. Yi, H. Yui, S. Asai, and M. Sumita. Selective location and double percolation of short carbon fiber filled polymer blends: high-density polyethylene/isotactic polypropylene. *Materials letters*, 36(Issues 1–4):186–190, July 1998.

[15] L. Shen, F. Q. Wang, H. Yang, and Q. R. Meng. The combined effects of carbon black and carbon fiber on the electrical properties of composites based on polyethylene or polyethylene/polypropylene blend. *Polymer testing*, 30:442–448, March 2011.

[16] J. Feng, C-H. Ming, and J-X. Li. A method to control the dispersion of carbon black in an immiscible polymer blend. *Polymer engineering and science*, 43:1058–1063, May 2003.

[17] O. Breuer, R. Tchoudakov, M. Narkis, and A. Siegmann. Segregated structures in carbon black-containing immiscible polymer blends: Hips/lldpe systems. *Journal of applied polymer science*, 64:1097–1106, October 1997.

[18] R. N. Rothon. *Particulate-filled polymer composites.* Smithers Rapra Technology, 2003.

[19] K. Nagata, H. Iwabuki, and H. Nigo. Effect of particle size of graphites on electrical conductivity of graphite/polymer composite. *Composite interfaces*, 6(5):483–495, April 1999.

[20] J. Feng and C-H. Ming. Double positive temperature coefficient effects of carbon black-filled polymer blends containing two semicrystalline polymers. *Polymer*, 41:4559–4565, June 2000.

[21] P. Potschke, B. Krause, S. Hermasch, R. Wursche, and R. Socher. Electrical and thermal properties of polyamide 12 composites with hybrid filler systems of multiwalled carbon nanotubes and carbon black. *Composites science and technology*, 71:1053–1059, 2011.

[22] A. E. Nesterov and Y. S. Lipatov. *Thermodynamics of polymer blends.* CRC Press, 1998.

[23] G. Wypych. *Handbook of fillers.* Chemtech publishing, 2016.

[24] J. V. Accorsi. The impact of carbon black morphology and dispersion on the weatherability of polyethylene. *Presented at International wire and cable symposium, Atlantic city*, 1999.

[25] W. Bauhofer and J. Z. Kovacs. A review and analysis of electrical percolation in carbon nanotube polymer composites. *Composites Science and Technology*, 69:1486–1498, June 2009.

[26] W. J. Kim, M. Taya, and M. N. Nguyen. Electrical and thermal conductivities of a silver flake/ thermosetting polymer matrix composite. *Mechanics of material*, 41:1116–1124, 2009.

[27] D. Pantea, H. Darmstadt, S. Kaliaguine, and C. Roy. Electrical conductivity of conductive carbon blacks: influence of surface chemistry and topology. *applied surface science*, 217:181–193, 2003.

[28] G. Lu, X. Li, H. Jiang, and X. Mao. Electrical conductivity of carbon fibers/abs resin composites mixed with carbon blacks. *Journal of applied polymer science*, 62:2193–2199, 1996.

[29] J. Sumfleth, X. C. Adroher, and K. Schulte. Synergistic effects in network formation and electrical properties of hybrid epoxy nanocomposites containing multi-wall carbon nanotubes and carbon black. *Journal of materials science*, 44:3241–3247, 2009.

[30] M. Drubetski, A. Siegmann, and M. Narkis. Electrical properties of hybrid carbon black/carbon fiber polypropylene composites. *Journal of materials science*, 42:1–8, 2007.

[31] M. Wen, X. Sun, L. Su, J. Shen, J. Li, and S. Guo. The electrical conductivity of carbon nanotube/carbon black/polypropylene composites prepared through multistage stretching extrusion. *Polymer*, 53(Issue 7):1602–1610, 2012.

[32] X. Zhang, G. Liang, J. Chang, A. Gu, L. Yuan, and W. Zhang. The origin of the electric and dielectric behavior of expanded graphite-carbon nanotube/cyanate ester composites with very high dielectric constant and low dielectric loss. *Carbon*, 50:4995–5007, 2012.

[33] S. M. Zhang, L. Lin, H. Deng, X. Gao, E. Bilotti, T. Peijs, Q. Zhang, and Q. Fu. Synergistic effect in conductive networks constructed with carbon nanofillers in different dimensions. *eXPRESS Polymer letters*, 6(No. 2):159–168, 2012.

[34] J. C. Grunlan, L. Liu, L. A. Hess, and K. C. Etika. The influence of synergistic stabilization of carbon black and clay on the electrical and mechanical properties of epoxy composites. *Carbon*, 47:3128–3136, 2009.

[35] P. Potschke and D. R. Paul. Formation of co-continuous structures in melt-mixed immiscible polymer blends. *Journal of macromolecular science Part C - Polymer reviews*, 43(1):87–141, 2003.

[36] Z. Tadmor and C. G. Gogos. *Principles of polymer processing*. Wiley, 2 edition, 2006.

[37] Y. Ngabonziza, J. Li, and C. F. Barry. Electrical conductivity and mechanical properties of multiwalled carbon nanotube-reinforced polypropylene nanocomposites. *Acta mechanica*, 220:289–298, April 2011.

[38] M. Sepe. Materials: Analyzing filler content. Website available at `http://www.ptonline.com/columns/materials-analyzing-filler-content`, 2015. Date of access: 2017-05-16.

[39] J. Goldstein, D. Newbury, D. Joy, C. Lyman, P. Echlin, E. Lifshin, L. Sawyer, and J. Michael. *Scanning Electron Microscopy and X-Ray Microanalysis*. Springer US, 2012.

[40] R. L. Blaine. Polymer heats of fusion. Website available at `http://www.tainstruments.com/pdf/literature/TN048.pdf`, 2003. Date of access: 2017-06-27.

APPENDIX A. RESULTS OF THE SURFACE RESISTIVITY MEASUREMENTS

Table 1 lists the individual samples' measurement data. Filler contents are listed in decreasing order from left to right, except data points, that are measured afterwards. For each material a median value and standard deviation are calculated.

Table 1 *Surface resistivity measurement data*

TP16597							
Content (wt-%)	19.6	15.6	13.7	11.7	10.8	9.8	-
Median (Ω)	1.5E3	4.0E3	3.0E5	2.0E7	2.0E8	1.0E12	-
St. Dev. (Ω)	1.2E4	8.5E4	2.0E5	2.1E8	4.3E10	0.0E0	-
1. sample (Ω)	3.0E4	2.0E5	5.0E5	1.0E7	1.0E11	1.0E12	-
2. sample (Ω)	2.0E3	4.0E3	1.0E5	5.0E8	9.0E7	1.0E12	-
3. sample (Ω)	1.0E3	4.0E3	1.0E5	3.0E7	3.0E8	1.0E12	-
4. sample (Ω)	1.0E3	4.0E3	5.0E5	6.0E6	5.0E7	1.0E12	-
TP16598							
Content (wt-%)	24.9	19.9	16.9	14.9	12.9	-	-
Median (Ω)	2.0E3	3.8E5	1.0E6	2.1E9	1.0E12	-	-
St. Dev. (Ω)	4.3E2	3.8E5	4.9E5	1.3E10	4.3E11	-	-
1. sample (Ω)	2.0E3	9.0E5	1.0E6	4.0E9	9.0E7	-	-
2. sample (Ω)	1.0E3	4.0E4	7.0E5	3.0E10	1.0E12	-	-
3. sample (Ω)	2.0E3	7.0E5	1.0E6	1.0E7	1.0E12	-	-
4. sample (Ω)	2.0E3	6.0E4	2.0E6	2.0E8	1.0E12	-	-
TP16599							
Content (wt-%)	12.1	8.1	7.0	6.5	6.0	5.0	-
Median (Ω)	5.0E4	5.5E4	1.0E5	2.0E5	8.0E5	1.0E12	-
St. Dev. (Ω)	4.3E3	1.2E4	4.7E4	1.5E5	5.7E5	0.0E0	-
1. sample (Ω)	5.0E4	8.0E4	2.0E5	5.0E5	2.0E6	1.0E12	-
2. sample (Ω)	5.0E4	6.0E4	1.0E5	2.0E5	1.0E6	1.0E12	-
3. sample (Ω)	5.0E4	5.0E4	8.0E4	1.0E5	6.0E5	1.0E12	-
4. sample (Ω)	4.0E4	5.0E4	1.0E5	2.0E5	6.0E5	1.0E12	-

Table 1 *Surface resistivity measurement data*

TP16600							
Content (wt-%)	33.8	31.8	29.8	28.8	27.9	26.9	25.9
Median (Ω)	6.5E4	1.0E5	6.0E5	1.0E6	9.0E6	6.0E8	3.3E11
St. Dev. (Ω)	1.2E4	4.3E4	2.1E5	8.8E5	1.0E6	8.5E9	4.1E11
1. sample (Ω)	7.0E4	1.0E5	1.0E6	9.0E5	8.0E6	2.0E8	6.0E11
2. sample (Ω)	6.0E4	1.0E5	5.0E5	1.0E6	8.0E6	1.0E9	5.0E10
3. sample (Ω)	9.0E4	2.0E5	5.0E5	1.0E6	1.0E7	2.0E8	2.0E9
4. sample (Ω)	6.0E4	1.0E5	7.0E5	3.0E6	1.0E7	2.0E10	1.0E12
TP16601							
Content (wt-%)	9.9	7.9	6.9	5.9	4.9	-	-
Median (Ω)	3.0E3	1.5E5	3.3E6	1.0E12	1.0E12	-	-
St. Dev. (Ω)	4.3E2	8.3E4	8.0E6	4.2E11	3.5E11		- -
1. sample (Ω)	3.0E3	2.0E5	2.0E7	2.0E10	1.0E12	-	-
2. sample (Ω)	2.0E3	1.0E5	5.0E5	1.0E12	1.0E12	-	-
3. sample (Ω)	3.0E3	1.0E5	3.0E5	1.0E12	1.0E12	-	-
4. sample (Ω)	3.0E3	3.0E5	6.0E6	1.0E12	2.0E11		- -
TP16602							
Content (wt-%)	16.0	14.0	12.0	11.0	10.0	9.0	-
Median (Ω)	7.5E3	2.4E5	3.0E5	6.0E6	3.0E11	1.0E12	-
St. Dev. (Ω)	6.1E3	2.3E5	3.3E5	2.6E6	3.7E11	0.0E0	-
1. sample (Ω)	5.0E3	4.0E5	1.0E6	8.0E6	1.0E11	1.0E12	-
2. sample (Ω)	5.0E3	6.0E5	4.0E5	4.0E6	1.0E11	1.0E12	-
3. sample (Ω)	2.0E4	7.0E4	2.0E5	1.0E7	1.0E12	1.0E12	-
4. sample (Ω)	1.0E4	7.0E4	2.0E5	4.0E6	5.0E11	1.0E12	-
TP16604							
Content (wt-%)	10.0	8.0	7.0	6.0	-	-	-
Median (Ω)	4.0E4	1.5E5	1.0E12	1.0E12	-	-	-
St. Dev. (Ω)	8.7E3	3.4E5	0.0E0	0.0E0	-	-	-
1. sample (Ω)	2.0E4	8.0E4	1.0E12	1.0E12	-	-	-
2. sample (Ω)	4.0E4	9.0E5	1.0E12	1.0E12	-	-	-
3. sample (Ω)	4.0E4	2.0E5	1.0E12	1.0E12	-	-	-
4. sample (Ω)	4.0E4	1.0E5	1.0E12	1.0E12	-	-	-
TP16605							
Content (wt-%)	33.9	30.0	29.0	28.0	27.0	26.0	-
Median (Ω)	8.0E5	5.0E6	9.0E6	4.5E7	1.3E11	1.4E9	-
St. Dev. (Ω)	2.0E5	3.6E6	5.3E6	1.1E7	3.1E11	1.5E9	-
1. sample (Ω)	6.0E5	1.0E7	2.0E7	3.0E7	8.0E11	2.0E9	-
2. sample (Ω)	1.0E6	2.0E6	9.0E6	4.0E7	2.0E11	4.0E9	-
3. sample (Ω)	6.0E5	8.0E6	9.0E6	6.0E7	6.0E10	3.0E7	-
4. sample (Ω)	1.0E6	2.0E6	6.0E6	5.0E7	4.0E10	7.0E8	-

Table 1 *Surface resistivity measurement data*

TP16681							
Content (wt-%)	20.7	19.7	18.6	16.6	-	-	-
Median (Ω)	1.4E5	7.5E5	3.6E8	1.0E12	-	-	-
St. Dev. (Ω)	6.8E4	1.5E6	2.2E10	0.0E0	-	-	-
1. sample (Ω)	5.0E4	4.0E5	7.0E8	1.0E12	-	-	-
2. sample (Ω)	2.0E5	8.0E5	1.0E7	1.0E12	-	-	-
3. sample (Ω)	2.0E5	4.0E6	1.0E7	1.0E12	-	-	-
4. sample (Ω)	8.0E4	7.0E5	5.0E10	1.0E12	-	-	-
TP16682							
Content (wt-%)	15.7	11.8	9.8	8.9	7.9	-	-
Median (Ω)	4.0E4	6.0E4	8.5E4	1.5E5	1.0E12	-	-
St. Dev. (Ω)	7.1E3	1.6E4	1.5E4	5.0E4	0.0E12	-	-
1. sample (Ω)	5.0E4	8.0E4	8.0E4	2.0E5	1.0E12	-	-
2. sample (Ω)	4.0E4	7.0E4	1.0E5	1.0E5	1.0E12	-	-
3. sample (Ω)	3.0E4	4.0E4	6.0E4	2.0E5	1.0E12	-	-
4. sample (Ω)	4.0E4	5.0E4	9.0E4	1.0E5	1.0E12	-	-
TP16683							
Content (wt-%)	20.0	15.0	10.0	8.0	-	-	-
Median (Ω)	3.0E4	4.5E4	1.0E12	1.0E12	-	-	-
St. Dev. (Ω)	4.3E3	5.0E3	0.0E12	0.0E12	-	-	-
1. sample (Ω)	4.0E4	5.0E4	1.0E12	1.0E12	-	-	-
2. sample (Ω)	3.0E4	4.0E4	1.0E12	1.0E12	-	-	-
3. sample (Ω)	3.0E4	5.0E4	1.0E12	1.0E12	-	-	-
4. sample (Ω)	3.0E4	4.0E4	1.0E12	1.0E12	-	-	-
TP16684							
Content (wt-%)	28.0	25.0	24.0	23.0	-	-	-
Median (Ω)	2.0E4	2.5E5	5.5E7	1,0E12	-	-	-
St. Dev. (Ω)	1.2E4	2.1E5	7.3E7	3.9E11	-	-	-
1. sample (Ω)	5.0E3	2.0E5	1.0E7	1.0E11	-	-	-
2. sample (Ω)	3.0E4	3.0E5	7.0E7	1.0E12	-	-	-
3. sample (Ω)	3.0E4	2.0E5	2.0E8	1.0E12	-	-	-
4. sample (Ω)	9.0E3	7.0E5	4.0E7	1.0E12	-	-	-
TP16685							
Content (wt-%)	14.2	13.2	12.2	11.2	10.2	-	-
Median (Ω)	6.0E4	3.5E5	2.0E5	1.0E12	1.0E12	-	-
St. Dev. (Ω)	7.1E3	3.8E5	4.3E4	1.7E11	0.0E0	-	-
1. sample (Ω)	6.0E4	1.0E6	2.0E5	1.0E12	1.0E12	-	-
2. sample (Ω)	7.0E4	1.0E5	1.0E5	1.0E12	1.0E12	-	-
3. sample (Ω)	5.0E4	6.0E5	2.0E5	1.0E12	1.0E12	-	-
4. sample (Ω)	6.0E4	1.0E5	2.0E5	6.0E11	1.0E12	-	-

Table 1 *Surface resistivity measurement data*

TP16686							
Content (wt-%)	16.5	14.5	13.6	12.6	11.6	10.7	-
Median (Ω)	1.3E4	2.0E5	3.0E6	5.0E8	5.0E11	1.0E12	-
St. Dev. (Ω)	1.5E4	1.2E5	1.2E7	2.2E10	5.0E11	0.0E0	-
1. sample (Ω)	3.0E3	4.0E5	2.0E6	1.0E6	1.0E12	1.0E12	-
2. sample (Ω)	2.0E4	8.0E4	3.0E6	1.0E9	2.0E7	1.0E12	-
3. sample (Ω)	5.0E3	2.0E5	3.0E6	3.0E6	1.0E12	1.0E12	-
4. sample (Ω)	4.0E4	2.0E5	3.0E7	5.0E10	1.0E7	1.0E12	-
TP16687							
Content (wt-%)	22.1	20.0	18.0	17.0	15.0	-	-
Median (Ω)	2.5E4	1.0E5	1.2E6	5.5E6	5.0E9	-	-
St. Dev. (Ω)	2.1E4	1.3E4	1.5E6	1.2E7	4.2E10	-	-
1. sample (Ω)	1.0E4	1.0E5	4.0E5	1.0E7	1.0E10	-	-
2. sample (Ω)	1.0E4	1.0E5	3.0E5	3.0E7	1.0E11	-	-
3. sample (Ω)	6.0E4	7.0E4	4.0E6	9.0E5	6.0E6	-	-
4. sample (Ω)	4.0E4	1.0E5	2.0E6	6.0E5	3.0E6	-	-
TP16688							
Content (wt-%)	16.0	14.0	11.0	10.0	-	-	-
Median (Ω)	6.0E4	6.0E6	5.5E11	1.0E12	-	-	-
St. Dev. (Ω)	2.4E5	1.3E8	3.3E11	0.0E0	-	-	-
1. sample (Ω)	5.0E4	5.0E6	3.0E11	1.0E12	-	-	-
2. sample (Ω)	6.0E4	3.0E8	2.0E11	1.0E12	-	-	-
3. sample (Ω)	6.0E5	2.0E6	1.0E12	1.0E12	-	-	-
4. sample (Ω)	6.0E4	7.0E6	8.0E11	1.0E12	-	-	-
TP16689							
Content (wt-%)	15.0	13.0	12.0	11.0	-	-	-
Median (Ω)	3.0E4	5.5E4	1.5E7	4.5E9	-	-	-
St. Dev. (Ω)	4.3E3	8.3E3	3.4E8	4.3E11	-	-	-
1. sample (Ω)	3.0E4	6.0E4	8.0E8	4.0E6	-	-	-
2. sample (Ω)	3.0E4	7.0E4	1.0E7	1.0E12	-	-	-
3. sample (Ω)	3.0E4	5.0E4	2.0E7	3.0E5	-	-	-
4. sample (Ω)	4.0E4	5.0E4	4.0E5	9.0E9	-	-	-
TP16690							
Content (wt-%)	30.0	24.0	22.0	20.0	18.0	-	-
Median (Ω)	1.0E4	7.0E5	4.6E8	9.5E9	2.4E11	-	-
St. Dev. (Ω)	4.9E3	1.1E6	1.6E9	4.3E11	1.8E11	-	-
1. sample (Ω)	1.0E4	3.0E6	1.0E7	2.0E9	4.0E11	-	-
2. sample (Ω)	2.0E4	1.0E6	8.0E6	1.0E12	3.0E10	-	-
3. sample (Ω)	7.0E3	4.0E5	9.0E8	9.0E9	4.0E11	-	-
4. sample (Ω)	1.0E4	4.0E5	9.0E8	9.0E9	4.0E11	-	-

Table 1 *Surface resistivity measurement data*

TP16691							
Content (wt-%)	18.2	16.2	15.2	14.2	12.1	-	-
Median (Ω)	2.5E4	6.5E4	6.5E5	4.0E6	1.0E12	-	-
St. Dev. (Ω)	8.3E3	7.0E4	7.2E5	3.3E6	3.9E11	-	-
1. sample (Ω)	3.0E4	3.0E4	2.0E5	1.0E7	1.0E12	-	-
2. sample (Ω)	3.0E4	3.0E4	3.0E5	5.0E6	1.0E11	-	-
3. sample (Ω)	2.0E4	2.0E5	2.0E6	1.0E6	1.0E12	-	-
4. sample (Ω)	1.0E4	1.0E5	1.0E6	1.0E6	1.0E12	-	-
TP16692							
Content (wt-%)	20.1	16.1	14.1	12.1	-	-	-
Median (Ω)	1.4E4	2.4E5	1.0E9	1.5E11	-	-	-
St. Dev. (Ω)	9.9E3	3.0E5	4.1E9	4.0E11	-	-	-
1. sample (Ω)	2.0E4	8.0E5	7.0E5	1.0E11	-	-	-
2. sample (Ω)	3.0E4	4.0E5	2.0E6	9.0E9	-	-	-
3. sample (Ω)	6.0E3	8.0E4	2.0E9	1.0E11	-	-	-
4. sample (Ω)	7.0E3	7.0E4	1.0E10	1.0E12	-	-	-
TP16739							
Content (wt-%)	20.9	18.8	17.8	16.8	-	-	-
Median (Ω)	2.8E5	3.5E7	1.0E8	2.0E9	-	-	-
St. Dev. (Ω)	2.2E5	8.2E7	4.1E8	4.3E11	-	-	-
1. sample (Ω)	5.0E4	2.0E5	1.0E6	6.0E6	-	-	-
2. sample (Ω)	6.0E4	2.0E5	4.0E5	1.0E7	-	-	-
3. sample (Ω)	5.0E5	2.0E8	1.0E9	4.0E9	-	-	-
4. sample (Ω)	5.0E5	7.0E7	2.0E8	1.0E12	-	-	-